Design and Testing for a Nontagged F1-V Fusion Protein as Vaccine Antigen against Bubonic and Pneumonic Plague

Bradford S. Powell,*,† Gerard P. Andrews,†,§ Jeffrey T. Enama,† Scott Jendrek,†,‡ Chris Bolt,† Patricia Worsham,† Jeffrey K. Pullen,†,⊥ Wilson Ribot,† Harry Hines,‖ Leonard Smith,‖ David G. Heath,† and Jeffrey J. Adamovicz†

United States Army Medical Research Institute of Infectious Diseases, Fort Detrick, Maryland 21702-1201

A two-component recombinant fusion protein antigen was re-engineered and tested as a medical counter measure against the possible biological threat of aerosolized *Yersinia pestis*. The active component of the proposed subunit vaccine combines the F1 capsular protein and V virulence antigen of *Y. pestis* and improves upon the design of an earlier histidine-tagged fusion protein. In the current study, different production strains were screened for suitable expression and a purification process was optimized to isolate an F1-V fusion protein absent extraneous coding sequences. Soluble F1-V protein was isolated to 99% purity by sequential liquid chromatography including capture and refolding of urea-denatured protein via anion exchange, followed by hydrophobic interaction, concentration, and then transfer into buffered saline for direct use after frozen storage. Protein identity and primary structure were verified by mass spectrometry and Edman sequencing, confirming a purified product of 477 amino acids and removal of the N-terminal methionine. Purity, quality, and higher-order structure were compared between lots using RP-HPLC, intrinsic fluorescence, CD spectroscopy, and multi-angle light scattering spectroscopy, all of which indicated a consistent and properly folded product. As formulated with aluminum hydroxide adjuvant and administered in a single subcutaneous dose, this new F1-V protein also protected mice from wild-type and non-encapsulated *Y. pestis* challenge strains, modeling prophylaxis against pneumonic and bubonic plague. These findings confirm that the fusion protein architecture provides superior protection over the former licensed product, establish a foundation from which to create a robust production process, and set forth assays for the development of F1-V as the active pharmaceutical ingredient of the next plague vaccine.

Introduction

The United States Department of Homeland Security and Department of Defense require an effective vaccine to protect against human plague. The new vaccine will also benefit the Centers for Disease Control and Prevention, state and local emergency response and rescue teams, as well as some scientists and members of the World Heath Organization who currently have no U.S. licensed plague vaccine for prophylaxis during laboratory and field work with *Yersinia pestis*. This paper describes the design, research level production, characterization, proof of concept testing, and comparative analysis of an improved fusion protein antigen that has been recommended by the United States Army Medical Research Institute of Infectious Diseases (USAMRIID) (*1*) as the active biological substance for the next plague vaccine.

Background. Plague is a zoonotic disease caused by *Y. pestis* that has impacted society, medicine, and military history. An estimated 200 million human deaths are attributable to plague through three recorded global pandemics and innumerable regional and local outbreaks. *Y. pestis* apparently emerged 15,000−20,000 years ago from its ancestor, *Yersinia pseudotuberculosis*, by acquiring and adapting genes for survival and increased virulence in both the flea and mammalian host (*2*−*5*). *Y. pestis* bacilli are typically transmitted among wild animals by fleas, thereby maintaining a natural reservoir as the sylvatic form of the disease. More than 200 mammalian species are known carriers or incidental hosts for *Y. pestis*, including humans and domestic and wild cats and dogs (*6*). Foci of epizootic disease continue to occur throughout the world today as plague is enzootic in semi-arid climates from the tropics to temperate zones. The World Health Organization tabulated a worldwide annual average of 2,547 human cases (15 in the U.S.) during a recent 10-year period (*7*). Contemporary outbreaks in India and East Africa and the increasing use of modern air travel have raised concern for possible global re-emergence of plague. Furthermore, the natural ability for gene transfer and documented occurrence of multi-drug-resistant strains (*4*, *8*, *9*) forewarns the ap-

* To whom correspondence should be addressed. Ph: +1-301-619-4933. Fax: +1-301-619-2152. E-mail: bradford.powell@amedd.army.mil.

† Division of Bacteriology, USAMRIID.

‖ Division of Toxinology, USAMRIID.

‡ Biopharmaceutical Development Program, SAIC Frederick, National Cancer Institute at Frederick, Frederick, MD 21702-1201.

⊥ Vaccine and Prevention Research Program, Division of AIDS, NIAID/NIH/DHHS, 6700B Rockledge Dr., Bethesda, MD 20892-7630.

§ Department of Veterinary Sciences, University of Wyoming, Laramie, WY 82070.

10.1021/bp050098r
Published on Web 08/09/2005

Report Documentation Page

Form Approved
OMB No. 0704-0188

1. REPORT DATE	2. REPORT TYPE	3. DATES COVERED
9 AUG 2005	**N/A**	**-**

4. TITLE AND SUBTITLE
Design and testing for a nontagged F1-V fusion protein as a vaccine antigen against bubonic and pneumonic plague, Biotechnology Progress 21:1490 - 1510

5a. CONTRACT NUMBER
5b. GRANT NUMBER
5c. PROGRAM ELEMENT NUMBER

6. AUTHOR(S)
Powell, BS Enama, JT Jendrek, S Ribot, W Bolt, C Pullen, JK Worsham, P Hines, H Smith, L Heath, DG Adamovicz, JJ Andrews, GP

5d. PROJECT NUMBER
5e. TASK NUMBER
5f. WORK UNIT NUMBER

7. PERFORMING ORGANIZATION NAME(S) AND ADDRESS(ES)
United States Army Medical Research Institute of Infectious Diseases, Fort Detrick, MD

8. PERFORMING ORGANIZATION REPORT NUMBER
RPP-05-183

9. SPONSORING/MONITORING AGENCY NAME(S) AND ADDRESS(ES)

10. SPONSOR/MONITOR'S ACRONYM(S)
11. SPONSOR/MONITOR'S REPORT NUMBER(S)

12. DISTRIBUTION/AVAILABILITY STATEMENT
Approved for public release, distribution unlimited

13. SUPPLEMENTARY NOTES

14. ABSTRACT

A two-component recombinant fusion protein antigen was re-engineered and tested as a medical counter measure against the possible biological threat of aerosolized Yersinia pestis. The active component of the proposed subunit vaccine combines the F1 capsular protein and V virulence antigen of Y. pestis and improves upon the design of an earlier histidine-tagged fusion protein. In the current study, different production strains were screened for suitable expression and a purification process was optimized to isolate an F1-V fusion protein absent extraneous coding sequences. Soluble F1-V protein was isolated to 99% purity by sequential liquid chromatography including capture and refolding of urea-denatured protein via anion exchange, followed by hydrophobic interaction, concentration, and then transfer into buffered saline for direct use after frozen storage. Protein identity and primary structure were verified by mass spectrometry and Edman sequencing, confirming a purified product of 477 amino acids and removal of the N-terminal methionine. Purity, quality, and higher-order structure were compared between lots using RP-HPLC, intrinsic fluorescence, CD spectroscopy, and multi-angle light scattering spectroscopy, all of which indicated a consistent and properly folded product. As formulated with aluminum hydroxide adjuvant and administered in a single subcutaneous dose, this new F1-V protein also protected mice from wild-type and non-encapsulated Y. pestis challenge strains, modeling prophylaxis against pneumonic and bubonic plague. These findings confirm that the fusion protein architecture provides superior protection over the former licensed product, establish a foundation from which to create a robust production process, and set forth assays for the development of F1-V as the active pharmaceutical ingredient of the next plague vaccine.

15. SUBJECT TERMS
Yersinia pestis, on-column refolding, protein aggregation, laboratory animals, mice

16. SECURITY CLASSIFICATION OF:			17. LIMITATION OF ABSTRACT	18. NUMBER OF PAGES	19a. NAME OF RESPONSIBLE PERSON
a. REPORT **unclassified**	b. ABSTRACT **unclassified**	c. THIS PAGE **unclassified**	**SAR**	**21**	

Standard Form 298 (Rev. 8-98)
Prescribed by ANSI Std Z39-18

pearance of plague cases that are increasingly difficult to treat by currently recommended antibiotic therapies (*10*).

Medical Aspects. Plague manifests as three principal disease forms in humans. Bubonic plague is the most frequent naturally acquired form of the disease and results from a flea bite in which *Y. pestis* bacilli are dispersed via the cutaneous lymphatic system. Lymph nodes nearest the site of entry become inflamed, forming painful buboes. The infection can spread throughout the body to cause secondary septicemic plague, associated with tissue necrosis at the extremities, and is usually fatal without antibiotic treatment (black death). Primary septicemic plague comes from direct infection of the blood stream and is also characterized by systemic toxicity with high risk for developing into secondary pneumonic plague. Primary pneumonic plague begins as a direct infection through the airway, acquired by inhaling respiratory droplets ejected from diseased animals or people, as can be broadcast by cough from up to 2 m. This form of the disease rapidly causes fever, cough, overwhelming sepsis, and shock. Survival from pneumonic plague requires antibiotic therapy within 24 h of exposure, often before specific knowledge of infection. Although plague can be recognized by clinical symptoms and diagnostic assays and post-exposure treatments are commonly available (*10*), successful intervention requires early action and strain susceptibility to the drug being administered. The most dependable medical countermeasure against plague is still prophylaxis with an effective vaccine.

Plague Vaccine. Plague is also a disease of military concern since it was used in warfare in the past and is considered a probable risk as a biological weapon for bioterrorism (*10*−*13*). It was present endemically or used intentionally during military conflicts dating back 4 millennia. Today, aerosolized *Y. pestis* presents a threat scenario of concern for public emergency planning and military safety because pneumonic plague is highly infectious, has a very rapid onset with high transmissibility and mortality, and is relatively easy to cultivate, genetically engineer, and weaponize. As recently as 1988, *Y. pestis* and other biological weapons agents were allegedly stockpiled for placement onto SS-18 missiles and targeting against major U.S. cities (*13*, *14*). Although the licensed Plague Vaccine USP may have helped to protect troops in the past against regional sylvatic plague (e.g., in Vietnam), it is no longer manufactured. Unlike its apparent success against bubonic plague, animal studies showed it to be ineffective against aerosol infection by wild-type strains or against infection by strains lacking capsule (*15*−*17*). Poor efficacy was surmised to be due to its reliance on an altered fraction 1 capsular antigen (F1 protein encoded by *caf1*) as primary immunostimulatory component, and the virtual absence of other known virulence factors as additional protective antigens (*15*). An experimental vaccine formulation containing purified F1 protein as the only antigen confirmed its ineffectual protection against lethal infection by strains lacking capsule (*15*−*17*). To correct these deficiencies, several other known *Y. pestis* virulence factors were screened for their ability to elicit protective immunity, and the low calcium response gene V product (V protein encoded by *lcrV*) demonstrated a high degree of protection in the mouse models for both bubonic and pneumonic plague (*16*, *18*, *19*). V is an effector protein that is transported into the eukaryotic host cell along with several other *Yersinia* outer proteins (YOPs) (*1*) by a contact-dependent Type III secretion system during infection (*20*). V protein serves a central role for pathogenesis as a regulator of the transfer of YOPs and is itself a modulator of innate immunity within the host cell (*21*, *22*). Absence of V in the former Plague Vaccine USP was suspected on the basis of the growth conditions used to produce the vaccine substance and then confirmed by anti-V immunoblot analysis of immune mice (*16*, *23*) and of the vaccine product itself (Andrews, G., unpublished data). In designing an improved plague vaccine, researchers at USAMRIID previously discovered that a subunit vaccine comprising a genetic fusion of recombinant F1 and V antigens protected mice very well against bubonic and pneumonic plague infection by virulent *Y. pestis* strains with or without F1 capsule (*17*). We report here an improvement on the original F1-V fusion protein design; the establishment of research-base methods for production and evaluation of purity, quality, and structure; and the demonstration of its high protective efficacy against bubonic and pneumonic plague as a candidate antigen for the next-generation plague vaccine.

Materials and Methods

Reagents and Strains. Chemicals and antibiotics were from Sigma-Aldrich (St. Louis, MO), except as specifically noted. Sterile, premixed Dulbecco's phosphate-buffered saline solution (DPBS) without calcium or magnesium was from Cambrex (Walkersville, MD) and EMD Chemicals, Inc. (Merck KGaA, Darmstadt, Germany). Both DPBS products pass quality control tests for low endotoxin before sale. Sterile, deionized water was supplied by a Solutions 2000 water purification system (Aqua Solutions, Jasper, GA). Bacto-Agar plate agar and premixed animal-product-free bacterial growth medium were from BD Diagnostics (Baltimore, MD). Laboratory preparations of Super broth and Terrific broth (*24*) were also formulated using, in place of tryptone, soy protein peptones that were manufactured with recombinant digestive enzymes (DMV International, Frazer, NY). Restriction enzymes, DNA polymerase, and DNA ligase were from New England Biolabs (Beverly, MA) except as specifically noted. *E. coli* B expression strains BL21 and BLR were from Novagen (Madison, WI) or from Cambrex Bio Science (Baltimore, MD) under service contract to USAMRIID as noted. Table 1 lists strains and plasmids used in this study. *E. coli* K-12 strain HMS 174 (DE3) (Novagen), harboring pLysS for added promoter control, and an HIS^+ cointegrate of *Pichia pastoris* strain GTS115 (*his4*) were tested as alternate host expression and production strains. To construct the *P. pastoris* strain, the F1-V gene fusion was cloned into the shuttle/suicide plasmid pHDL4 (gift from the Phillips Petroleum Company, Bartlesville, OK) by service contract (Intracel, Frederick, MD) using synthetic genes assembled from oligonucleotides. For studies of vaccine effectiveness, laboratory stocks of *Y. pestis* CO92 (wild-type) and C12 (non-encapsulated mutant) were cultivated as previously described (*17*). Proteins used for comparisons were obtained from the following sources: the former fusion protein His_{10}-F1-V protein and F1 protein were purified in the laboratory as described (*15*, *17*); protease-cleaved recombinant V protein (rV) (*17*) and the first pilot batch of F1-V from strain BL21 (DE3)/pPW731 were provided by service contract (PerImmune); and F1-V fusion proteins expressed in *E. coli* HMS and *P. pastoris* were purified by an abbreviated process comprising a small-scale version of Step 1 and Step 4 described herein. Unpolished F1-V hold material purified from strain BLR (DE3)/pPW731 by a different process under contract was supplied to USAMRIID via DVC (Frederick, MD) for plague vaccine bridging studies. All other stocks of F1-V

Table 1. Strains Used in This Study

strain, plasmid	genotype, phenotype	recombinant product	ref/source
	Escherichia coli		
HB101	F$^-$ *leu*B6, *pro*A2, *rec*A13, *thi*-14, *ara*-14, *lac*Y1, *gal*K2, *xyl*-5, *mtl*-1, *rps*L20, *sup*E44, *hsd*S20		lab stock
BL21	*E.coli* B, F$^-$ *ompT hsdS$_B$*($r_B^-m_B^-$) *gal dcm*		Novagen
BL21 (DE3)	BL21λ (DE3)		Novagen
HMS174 (DE3)	*E.coli* K12, F$^-$ *ompT hsdR*($r_{K12}^-m_{K12}^+$) λ(DE3), Rif^R Cm^R		Novagen
BLR	BL21 λ(DE3) Δ*(slr-recA)306::*Tn*10* Tet^R		Novagen[a]
pHis-F1-V	pET19bΩ(*caf1-EcoRI-lcrV*), Amp^R	His$_{10}$ -F1-V, original construct	17
pMF1-V 4	pET24aΩ(*caf1-EcoRI-lcrV*), Amp^R	*caf1* without leader, errors still in *lcrV*	this work
p6189A	pNoTA/T7Ω(*EcoRI-lcrV-SalI*)	*lcrV* from *Y. pestis* Antigua	this work
MF1-V 8192[b]	BL21(DE3)/pET28aΩ(*caf1-EcoRI-lcrV*), Kan^R	His$_6$-F1-V	this work
pPW731 (alias pMF1-V 731)[b]	pET24aΩ(*caf1-EcoRI-lcrV*), Kan^R	F1-V[b]	this work
HB101/pBRF1[c]	pB*R*322Ω(*caf1*), Amp^R	F1	15
BL21/plcrV[d]	pET15bΩ(*lcrV*), Amp^R	rV	17
	Pichia pastoris		
GTS115	*his4*, His$^-$		lab stock
pHIDL4	His$^+$		Phillips Petroleum Co.
GTS115::pHIDL4-F1-V	His$^+$	F1-V	this work
	Yersinia pestis		
CO92	F1$^+$		58
C12[e]	*caf1*, F1$^-$		59

[a] Final production strain BLR/pPW731 was provided by Cambrex BioScience Inc. during cell banking by service contract to USAMRIID. [b] In the modified F1-V fusion construct, designated by the name prefix "M," two silent point mutations in the *lcrV* coding sequence of the original pHis$_{10}$-F1-V are corrected back to wild-type, and the leader sequence of *caf1* is removed. The final production plasmid, pPW731, expresses the modified F1-V fusion protein with no extraneous amino acid sequence tags. [c] Recombinant F1 is translated with its natural signal sequence, which is removed during expression in *E. coli* to produce a natural-sized F1 protein of 15,694 Da (*15*). [d] Recombinant V protein (rV) is expressed as a His$_6$-V product. During purification, the histidine tag is cleaved to yield a final putative protein containing three additional N-terminal amino acids (GSH...) and calculated mass of 37,521 Da (*17*). [e] *Y. pestis* C12 is derived from strain CO92 and contains stop codons replacing the first two coded amino acids of the F1 capsule structural gene (*caf1*), eliminating capsule production and rendering an F1$^-$ phenotype.

were prepared at USAMRIID as described below. Rabbit polyclonal antibodies used for detection of F1-V protein by immunoblot were generated using purified F1 and purified rV protein antigens and standard protocols. Rabbit anti-F1 antiserum from animal no. 716A was adsorbed to *E. coli* protein to remove cross-reacting activity. Rabbit anti-V IgG from animal no. 04527 was purified by liquid chromatography over Protein-A Sepharose (Amersham Biosciences, Piscataway, NJ) to a final stock concentration of 7.8 mg/mL. Plague Vaccine USP was obtained from Greer Laboratories (Lenoir, NC).

Engineering the Expression Plasmid. The original His$_{10}$-F1-V construct was built on the expression plasmid pET-19b (Novagen) and contained the complete *caf1* gene joined on the 3′ side to the *lcrV* gene through an *Eco* RI junction (coding for an in-frame glutamate-phenylalanine dipeptide linker). The 5′ region contained 23 additional codons, including 10 histidines and an enterokinase cleavage site as designed, but the *lcrV* gene contained two inadvertent point mutations that changed one amino acid (*17*). Therefore, the original His$_{10}$-tagged F1-V product contained 521 amino acids with a predicted mass of 57,926 Da (*17*). To obtain a new fusion without N-terminal tags or F1 leader sequence and with corrected V sequence, the *caf1-EcoRI-lcrV* region was modified in two stages. First, the N-terminal tags and leader sequence region of *caf1* were eliminated while subcloning from the pET-19b-His$_{10}$-F1-V clone via PCR with forward primer 5′-GACTGCTCATATGGCAGATTTAACTG-CAAGCACC-3′ and reverse primer 5′-GCGGGATCCT-CATTTACCAGACGTGTC-3′ (*Nde* I and *Bam*H I restriction endonuclease sites underlined). The amplified fragment was purified by agarose gel electrophoresis, digested with restriction enzymes *Nde* I and *Bam*H I, repurified by gel, and then ligated into plasmid pET-24a (Novagen), previously cut with *Nde* I and *Bam*H I. Resulting plasmid clones were sequenced to confirm identity with the template DNA sequence. Plasmid pET-24a-*caf1-EcoRI-lcrV* (called MF1-V clone no. 4) was cut with *Eco*R I and *Sal* I to remove the aberrant *lcrV*, and the vector fragment containing *caf1* was gel purified for further use as described below. A new *lcrV* coding region, flanked by *Eco*R I and *Sal* I sites, was produced by PCR using HF-Advantage high-fidelity polymerase (Clontech, Palo Alto, CA) and oligonucleotide primers (forward, cgcgaattcatgattagagcctacgaac; reverse, tacgtcgactcatttac-cagacg-tgtcatctagcagon) using *lcrV* clone no. 184 as source DNA. Clone no. 184 was previously cloned into pET-15b using DNA from *Y. pestis* Antigua strain (Strachan, S., unpublished results). This new *lcrV* coding sequence was cloned into pNoTA/T7 (5 Prime → 3 Prime, Boulder, CO) as an intermediate holding vector. The expected nucleotide sequence was confirmed as the consensus for *lcrV* (*3*, *25*) by sequencing both strands, and this plasmid clone was designated p6189A. Plasmid p6189A DNA was isolated and cut with *Eco* R1 and *Sal* I, and the fragment containing *lcrV* was purified by agarose gel electrophoresis and ligated into the vector fragment of Clone no. 4 containing the leaderless *caf1* described above. The ligation mix was transformed into competent NovaBlue cells (Novagen), a nonproduction strain, to ensure plasmid stability. The final plasmid construct was designated pMF1-V 731 (alias pPW731). The entire *caf1* and *lcrV* genes, as well as junction regions, were determined to be correct by RFLP analysis and by sequencing both strands. Plasmid pPW731 was transformed into the production strains BL21 (DE3), BL21 (DE3)/pLysS and HMS174 (DE3) for preliminary testing and then transformed into the *recA* strain BLR (DE3) for cell banking, process development, and later production runs.

To investigate production of the F1-V vaccine in the *P. pastoris* expression system, synthetic genes for *caf1* and *lcrV* were engineered using nine gel-purified oligonucleotides of ca. 74 bases with 24-base overlap. Both genes were first optimized for preferred codons of *P. pastoris*, uniformly reducing the AT content of the native genes down to 48% GC and removing potential rare codons across both coding regions. Unique restriction sites were added for use in fusing F1 and V genes together and inserting into the yeast expression plasmid, pHILD4. Separate gene fragments, comprising *Eco R*I-*caf-Apo* I and *Apo* I-*lcrV-Hind* III, were amplified by PCR using Vent polymerase, inserted into the pHILD4 plasmid, and transformed into an *E. coli* DH5α host. The *Apo* I site (GAATTT) used for gene fusion adds a glutamate-phenylalanine dipeptide linker to the translation product. After confirming the expected nucleotide sequence, the resulting pHILD4-F1-V shuttle plasmid was linearized with the restriction enzyme *Sst* I and transformed into *P. pastoris* GS115 by electroporation with selection for kanamycin resistance and subsequent isolation of exconjugates on histidine-deficient medium. Stock seed cultures were prepared for protein expression by cultivation on basal fermentation medium plus PTM_4 trace mineral salts with 2% glycerol as described previously (*26*).

Cell Banking. Research and development expression strain BL21(DE3)/pPW731 was grown in medium free of animal products and with antibiotics as described below and then stored in 12% glycerol at −70 °C. The process development cell bank comprising production strain BLR (DE3)/pPW731 was prepared and banked by contract to USAMRIID (Cambrex Bio Science) and passed quality control testing specifications for culture purity (colony morphology), microbial identity (*E. coli*), plasmid stability (90%), and pre- and post-freezing viable counts (6×10^8 cfu/mL).

Fermentation and Capture. The F1-V expression strains were grown in a Micros I top-drive fermentor (New Brunswick Scientific, New Brunswick, NJ) equipped with a model 316L stainless steel vessel of 20-L working volume plus two Rushton impellers, a two-gas mixer, polarographic dissolved oxygen (DO_2) probe (Ingold, Wilmington, Pa), gel-filled pH probe (Ingold), and an ML4100 process controller with Advanced Fermentation software (New Brunswick Scientific). For fermentation seed, duplicate pre-cultures were prepared by inoculating a 50-μL aliquot of frozen glycerol stock into shake flasks containing 500 mL of sterilized 1X Terrific Broth and supplemented with antibiotics as appropriate for the expression strain: ampicillin (100 mg/L) or carbenicillin for strain BL21(DE3)/pPW731; kanamycin (30 mg/L) and tetracycline (15 mg/L) for strain BLR (DE3)/pPW731. The pre-cultures were adjusted to pH 7.1 using 2 M NaOH and grown at 37 °C, 200 rpm, for 10 h or until reaching an optical density at 550 nm (OD_{550}) of ∼3.74. Subsequently, all 500 mL from one of the pre-cultures was transferred to the sterilized fermentor containing 19.5 L of the same medium and antibiotics, pre-equilibrated at 100% DO_2, 37 °C, 500 rpm, and positive vessel pressure. Measurements of OD_{550}, DO_2, online/offline pH, temperature, vessel pressure, agitation, and airflow were monitored hourly until induction. A pH of 7.1 was maintained with 2 M NaOH using a controller, and a DO_2 of 40% was maintained using a gas feed supplemented with an oxygen controller. A feed of Terrific Broth 392 g/L + glycerol (170 g/L) was started prior to inducing at an OD_{550} of 23.3 (5 h) with 1 mM dioxanes-free IPTG, at which point vessel controls were monitored every 15 min for another 2 h. The fermentor was chilled to 10 °C by a cold water jacket at an OD_{550} of 33, and cells were collected with a peristaltic pump at 25 L/h through the fermentor harvest valve into a CEPA LE continuous-flow centrifuge (New Brunswick Scientific) equipped with a clarification bowl and centrifuged at 40,000 × *g*. Cell paste was collected into plastic bags in 100-g increments (600 g total per 20 L fermentation) and stored at −70 °C until use. *Pichia pastoris* strain GTS115/pHILD4-F1-V was fermented using basal medium with PTM_4 trace mineral salts and three staged feeds of glycerol and methanol as previously described (*26*).

Cells were cracked open and clarified in 100 g amounts, or as stated otherwise, to provide source material for process development and for final demonstration runs. Frozen cell paste was thawed by immersion in cold water and thoroughly re-suspended in cracking buffer (20 mM ethanolamine pH 9.5, 2 mM EDTA) to a final volume of 250 mL. Cells were broken by four consecutive passages through a model 110Y Micro-fluidizer (Microfluidics, Newton, MA) at 90 psi cycle pressure with 20,000−21,000 pounds back pressure and then sonicated three times on ice with 25 × 1 s pulses at 50% duty (Sonic Materials Vibra Cell, Sonics, Newtown, CT). Cell debris was cleared by two consecutive centrifugations at 11,000 × *g* for 30 min in a Beckman Coulter Avanti J-25 centrifuge (Fullerton, CA). For purification runs, clarified supernatant (ca. 175 mL) was processed immediately beginning with Step 1 below.

Purification Step 1: Recovery and Refolding. Anion exchange chromatography (AEX) was used to capture and refold F1-V as the first optimized step of F1-V purification (see Results section regarding salting out procedures). A Fineline Pilot 35 column was packed with Source 15Q resin (Amersham Biosciences) to a final bed volume of 152 mL and connected to an Äkta Explorer high pressure liquid chromatography (HPLC) system equipped with Frac-950 fraction collector (Amersham Biosciences). Mobile phase buffers, Buffer QA (20 mM ethanolamine pH 9.5, 2 mM EDTA) and Buffer QB (20 mM ethanolamine pH 9.5, 2 mM EDTA + 1 M NaCl), were prepared, filtered, and primed into pumps A1 and B1 as supply for programmed method buffers "A" and "B," respectively. Loading Buffer (Buffer QA + 6 M urea), prepared and filtered similarly, was primed into pump A2 for sample loading and washing away unbound sample. The column was washed, charged, equilibrated at the method flow rate of 10 mL/min using 5 column volumes (CV) water, 1 CV of Buffer QA, 1 CV of Buffer QB, 1 CV of Buffer QA, and then equilibrated with 1 CV of Loading Buffer. Sample was prepared at room temperature by slowly adding finely ground urea with gentle stirring to a final concentration of 6 M and volume of 250 mL. This load material was processed all at once (large scale) or in two batches (smaller scale) with storage of half at 4 °C for similar processing the next day. Sample material was sonicated using the same procedure described for lysis above and then loaded onto the column using a 150-mL super loop. During injection, the superloop was washed using 1 CV of Loading Buffer through line A2, followed by 4 CV of method Buffer A (i.e., QA in line A1), collecting nonbinding material in 500-mL bottles. F1-V was eluted with the following programmed method: 3.5 CV to 8% B; 4 CV to 30% B; 0.6 CV to 40% B; 0.2 CV to 100% B; 1.5 CV at 100% B; 0.1 CV to 0% B; 1 CV at 0% B; collecting 45-mL fractions into 50-mL Falcon conical screw-cap tubes (BD Biosciences, San Jose, CA) throughout the run and storage at 4 °C during analysis by SDS−PAGE and immunoblot as described

001 MADLTASTTA TATLVEPARI TLTYKEGAPI TIMDNGNIDT ELLVGTLTLG GYKTGTTSTS VNFTDAAGDP MYLTFTSQDG NNHQFTTKVI GKDSRDFDIS
101 PKVNGENLVG DDVVLATGSQ DFFVRSIGSK GGKLAAGKYT DAVTVTVSNQ **EF**MIRAYEQN PQHFIEDLEK VRVEQLTGHG SSVLEELVQL VKDKNIDISI
201 KYDPRKDSEV FANRVITDDI ELLKKILAYF LPEDAILKGG HYDNQLQNGI KRVKEFLESS PNTQWELRAF MAVMHFSLTA DRIDDDILKV IVDSMNHHGD
301 ARSKLREELA ELTAELKIYS VIQAEINKHL SSSGTINIHD KSINLMDKNL YGYTDEEIFK ASAEYKILEK MPQTTIQVDG SEKKIVSIKD FLGSENKRTG
401 ALGNLKNSYS YNKDNNELSH FATTCSDKSR PLNDLVSQKT TQLSDITSRF NSAIEALNRF IQKYDSVMQR LLDDTSGK

Figure 1. Amino acid sequence of the F1-V fusion protein. Predicted amino acid sequence of the putative 478 amino acid F1-V translation product from the *caf1-EcoRI-lcrV* gene fusion (GenBank accession number AY924380) carried on pPW731 is shown. Recombinant dipeptide junction between F1 and V is shown in boldface. Edman degradation sequencing revealed an N-terminus of ADLTASTTAT. Tryptic peptides and amino acids confirmed experimentally by ESI-LC/MS/MS (Figure 5) and covering 89% of the total sequence are shown in normal type; those not observed are underlined. An observed whole protein mass of *m/z* 53,034 measured by MALDI-TOF-MS (Figure 4) concurs with the calculated mass of 53,061 for the 477 amino acid, des-Met protein product.

below. Fractions containing F1-V (11−23% B) were pooled for immediate application of purification Step 2.

Purification Step 2: Further Purification. For smaller-scale purifications, an HiPrep Butyl FF 16/10 hydrophobic interaction chromatography (HIC) column (CV = 20.1 mL) (Amersham Biosciences) was washed at the method flow rate of 5 mL/min with 1 CV of deionized water, and then pumps A1 and B1 were primed with Buffer OA (HIC method buffer A = 1 M ammonium sulfate in 20 mM ethanolamine pH 9.5, 2 mM EDTA) and Buffer OB (HIC method buffer B = 20 mM ethanolamine pH 9.5, 2 mM EDTA), respectively. The column was equilibrated with 1 CV of Buffer OB and then with 2 CV of Buffer OA until achieving stable conductivity baseline. Half of the F1-V pool from Step 1 was adjusted to match the starting buffer conductivity using a 2X stock of Buffer OA and a conductivity meter (model 604, Amber Science Inc, Eugene, OR) and then loaded onto the column through the sample pump using the "Direct Load" application of the Äkta Explorer instrument. F1-V was eluted with the following programmed method: 2 CV at 0% B; 10 CV to 100% B; and 5.5 CV at 100% B; collecting 5-mL fractions across the entire gradient. Fractions (25−90% B) were assayed as described above.

For larger-scale HIC, a Bioprocess XK50 column (Amersham Biosciences) was packed with Butyl Sepharose 4 Fast Flow resin (Amersham Biosciences) to a final bed volume of 992 mL. The column was equilibrated at the method flow rate of 15 mL/min using the following wash sequence: 2 CV of Buffer OA, 1 CV of Buffer OB, 1 CV of Buffer OA. The pooled F1-V load sample was adjusted as described above, then loaded onto the column using the sample pump ("Direct Load"), and eluted by the following programmed method: 0.25 CV to 90% B; 1 CV at 90% B; 0.2 CV to 100% B; and 3 CV at 100% B; collecting 250-mL fractions into 250-mL glass screw-cap bottles (Corning Inc., Acton, MA), with the collector in "Prep Mode." Fractions were analyzed by SDS page as before, and fractions containing F1-V were pooled for immediate concentration (Step 3) or held overnight at 4 °C if necessary.

Purification Step 3: Concentration. F1-V was concentrated by HIC using the same HiPrep Butyl FF 16/10 column and similar buffers described above except method Buffer A contained ammonium acetate instead of ammonium sulfate. Buffer AA (1 M ammonium acetate in 20 mM ethanolamine pH 9.5, 2 mM EDTA) and Buffer AB (20 mM ethanolamine pH 9.5, 2 mM EDTA) were prepared and primed into pumps A1 and B1, and the column was washed at the method flow rate of 5 mL/min with 1 CV of deionized water and then equilibrated using 1 CV of Buffer AA, 1 CV of Buffer AB, and Buffer AA to stable conductivity baseline. The conductivity of the pooled sample from Step 2 was adjusted by very slowly adding 2X AA stock with gentle stirring at room temperature, then applied by direct load through a sample pump, and eluted with the following programmed method: 2 CV at 0% B; 0.2 CV to 100% B; and 4 CV at 100% B; collecting 5-mL fractions across the gradient. The fractions were assayed using SDS−PAGE, and fractions containing F1-V were pooled for buffer exchange, Step 4.

An alternative method for concentration employing AEX instead of HIC was also developed because of occasional losses from salting out (see Results below). The pooled F1-V sample to be concentrated was first diluted with deionized water to reduce conductivity to match that of the load buffer, Buffer QA (above). The adjusted sample was then loaded onto a 6-mL Resource Q column (Amersham Biosciences), previously washed and equilibrated at 6 mL/min with 5 CV of deionized water, 1 CV of QA, 1 CV of QB (as above), and again with 3 CV of QA. F1-V was eluted from the column in a rapid gradient by the following programmed method: 3 CV at 0% B; 0.2 CV to 30% B; 5 CV at 30% B; 0.2CV to 100% B; and 2 CV at 100% B, collecting 5-mL fractions for analysis and pooling as described above.

Purification Step 4: Buffer Exchange. Two 26 mm × 100 mm HiPrep 26/10 (Amersham Biosciences) desalting columns (combined CV = 106 mL total) were connected in series, washed with 2 CV of deionized water, and then equilibrated with DPBS at the method flow rate of 10 mL/min just before use. Pooled F1-V was loaded using a 50-mL superloop at less than 20 mL per run (3 runs typically) and eluted with 1.5 CV, and 10-mL fractions were collected into 15-mL Falcon tubes. Peak fraction appeared at 38 mL elution volume and was filtered using Millex-GV (Millipore, Beverly, MA) 0.22-μm syringe filters at a single pass per filter. The final pool was distributed into 1-mL volumes into pre-labeled 1.5-mL cryo-storage tubes (Nalge Nunc International, Rochester, NY), snap frozen on dry ice in ethanol, and finally stored at −70 °C until needed. Protein concentration was determined by the BCA microtiter plate method using BSA standards as described by the product vendor (Pierce).

All chromatographic columns used in the final optimized purification process, from Step 1 through Step 4, were cleaned to remove endotoxin before use as follows: 1 CV of deionized water, 1 or more CV of 0.5 N NaOH to exceed 1 h on column, and 1 CV of 0.1 N NaOH for storage and hold until next use, which was preceded with 5 CV of deionized water before charging and equilibration. All mobile phase buffers for preparative and analytical chromatography were clarified through bottle-top filters with either 0.22 μm cellulose acetate membrane (Corning) or 0.2 μm nylon membrane (Nalge Nunc) as appropriate for aqueous- or organic-containing solutions.

DNA and Endotoxin. F1-V lots were assayed for DNA contamination by fluorescence spectroscopy of Hoechst 33258 dye (Sigma-Aldrich) essentially as previously described (*27*), using a model LS 50B luminescence

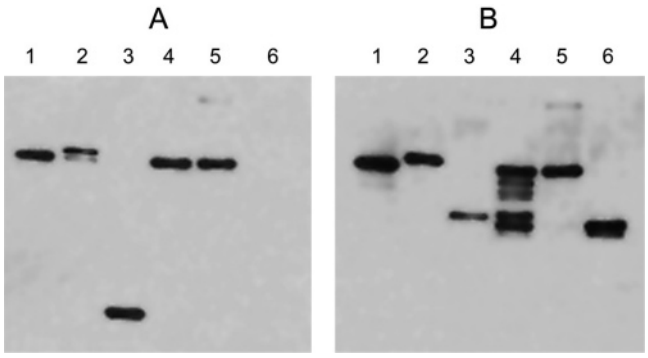

Figure 2. Immunoblot scouting for F1-V quality from potential production strains. Proteins fractionated by SDS−PAGE and transferred to nitrocellulose were detected separately with anti-F1 antibodies (A) or anti-V antibodies (B). Sample identities by lane: (1) initial extraction of F1-V from *E. coli* BL21 (DE3)/pPW731 clone; (2) His_{10}-F1-V fusion protein *(17)*; (3) cocktail of individual recombinant F1 and V proteins; (4) F1-V from *E. coli* HMS 174 (DE3)/pLysS pPW731; (5) first production lot of F1-V from *E. coli* BL21 (DE3)/pPW731; (6) F1-V from *P. pastoris*. Calculated masses for the purified proteins F1, 15,694; V, 37,-240; His_{10}-F1-V, 55,960; F1-V, 53,061 (see note to Figure 1).

spectrometer according to instructions of the vendor (Perkin-Elmer, Boston, MA). Endotoxic activity from residual lipopolysaccharide contamination was measured by the *Limulus* amoebocyte lysate (LAL) assay using the E-Toxate kit as prescribed (Sigma) or via service contract to USAMRIID (Cambrex) using the Kinetic-QCL test as performed in accordance with Food and Drug Administration (FDA) Guidelines.

SDS−PAGE and Immunoblot. Instruments, supplies, reagents and software for sodium dodecyl sulfate−polyacrylamide gel electrophoresis (SDS−PAGE) and gel image analysis were used as described by the vendor (Bio-Rad Laboratories, Hercules, CA). Gels were thoroughly rinsed in deionized water, stained with colloidal Coomassie Blue dye using GelCode Blue, and destained as prescribed by the vendor (Pierce Biotechnologies Inc., Rockford, IL). Gel images were captured with an HP Scanjet 7400C document scanner (HP, San Jose, CA) for storage as JPEG files. Relative band intensities were measured by densitometry using either the model GS-700 imaging densitometer (BioRad) or using a Flour S Max_2 cooled CCD video camera with QuantityOne software (BioRad). For immunoblots, proteins from identical duplicate sets of SDS−PAGE gels were transferred to pre-cut nitrocellulose membranes as described by the vendor of the membranes and Criterion Blotter transfer apparatus (Bio-Rad). After blocking overnight (DPBS, 0.5% gelatin, 0.1% Tween-20), F1 and V proteins were probed simultaneously using an optimized mixture of rabbit polyclonal antibodies (anti-F1 antiserum at 1:50,-000 dilution and anti-V IgG at 1:200,000 dilution) for 1 h. Membranes were washed 3 × 15 min (DPBS, 0.1% Tween-20), treated with secondary antibody (1:2000 dilution) alkaline phosphatase-labeled goat anti-rabbit IgG (KPL, Gaithersburg, MD) for 1 h at room temperature, washed as before, and then stained with the premixed colorimetric dye 1-Step NBT/BCIP (Pierce) for 30 s to 30 min as needed. The reaction was stopped with deionized water, and an image of freshly dried membrane was captured as described above. For early evaluation of F1-V isolates from candidate production strains, immunoblots were visualized using ECL chemiluminescence detection as prescribed by the vendor (Amersham Biosciences).

CIEF. Isoelectric point of purified F1-V protein was measured by capillary isoelectric focusing (CIEF) using reagents and software of the BioFocus instrument as described by the vendor (BioRad).

RP-HPLC. Reversed-phase high-pressure liquid chromatography (RP-HPLC) was performed on an Äkta 10 Explorer liquid chromatograph (Amersham) in organic phase mode using a POROS R2/M 4.6 × 100 mm column (CV = 1.662 mL) at 10 mL/min flow rate. This column is now available as "POROS 20 micron" from Applied BioSystems (Foster City, CA). Sample was carefully diluted 1:1 in mobile phase Buffer A, degassed and clarified through a 0.2-μm syringe filter (Corning), loaded into a 100-mL sample loop, and then separated with filtered mobile phase Buffer A (5% acetonitrile, 0.1% HCl) and Buffer B (95% acetonitrile, 0.1% HCl) by the following programmed method: 5 CV at 0% B; 20 CV to 100% B; 2 CV at 100% B; 5 CV to 0% B.

CD Spectroscopy and Secondary Structure Calculations. The content of α-helix, random coil, and β-sheet secondary structures for F1-V was measured experimentally and compared to model-generated computer predictions. Far-UV circular dichroism (CD) spectra were collected at room temperature on a JASCO J-810 spectropolarimeter as prescribed by the vendor (JASCO, Great Dunmow, UK). Samples from various lots were diluted to 50 μg/mL using 10 mM sodium phosphate buffer pH 7.2, filtered through a 0.2-μm syringe filter, and held at room temperature before analysis. Measurements were performed using standard sensitivity, continuous mode scan from 260 to 180 nm at 20 nm/min with 1 s time constant, 0.5 nm pitch and averaged from 10 accumulations. Scan data were averaged and converted to molar ellipticity using the instrument software. A consensus from eight predicted secondary structures was obtained for F1-V, F1 and V amino acid sequences by the method of Combet (*28*), as accessible on the interactive web site http://npsa-pbil.ibcp.fr.

Intrinsic Tryptophan Fluorescence Spectroscopy. Variance in tertiary structure between lots of F1-V was measured by intrinsic tryptophan fluorescence spectroscopy on a model LS 50B luminescence spectrometer as specified by the vendor (Perkin-Elmer) using an emission spectrum from 300 to 400 nm at a scan speed of 20 nm/min, 295 nm excitation wavelength, and 3 nm slit widths. Samples were prepared as for CD spectroscopy, and data were compared in the spectral range from 320 to 400 nm.

Mass Spectrometry and Amino Acid Sequencing. Whole protein mass of purified F1-V protein was analyzed by matrix-assisted laser desorption/ionization mass spectrometry (MALDI-TOF-MS), and amino acid sequence was analyzed by liquid chromatography electrospray ionization tandem mass spectrometry (LC-ESI/MS/MS). MALDI-TOF-MS was carried out on an externally calibrated Applied Biosystems Voyager-DE mass spectrometer (Framingham, MA) essentially as described previously with minor changes (*29*). For a typical experiment, 5 μM final concentration of protein was mixed with 150 mM NaCl in 10 mM potassium phosphate pH 7.0 buffer. After 30 min at 37 °C, 5 μL was added to 3 μL of matrix (10 mg/mL sinapinic acid in 50% acetonitrile, 0.02% trifluoroacetic acid (v/v)) for a 1.67:1 protein-to-matrix ratio (v/v), and 1 μL was spotted onto a stainless steel sample plate. Spectra were acquired in delayed extraction mode with the following operating conditions: an accelerating voltage of 25 kV, a grid voltage of 93.2%, and a guide wire voltage of 0.3%. The scanned mass range was *m/z* 2,000 to approximately 380,000, and 128 scans were averaged to yield each spectrum. The

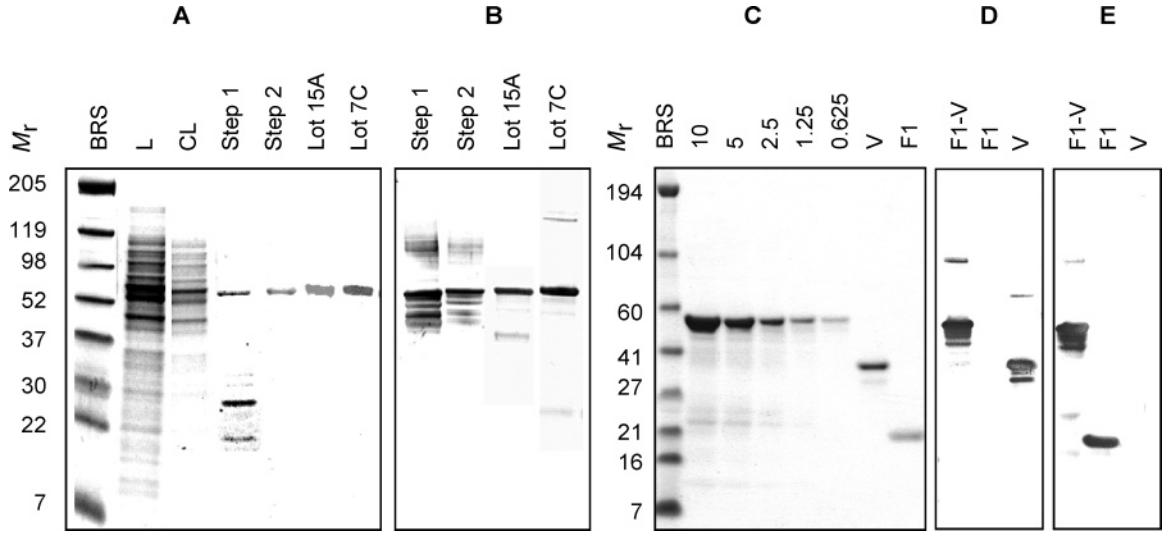

Figure 3. SDS−PAGE and immunoblot analysis of F1-V during stages of purification. Proteins separated by SDS−PAGE, 4−12% T, in Tris-HCL glycine running buffer (panels A and B) or in MES running buffer (panels C−E) and detected by Coomassie Blue stain or immunoblot as follows: (A) stain of F1-V production summary gel; (B) immunoblot of purified F1-V using cocktail of rabbit polyclonal anti-F1 and anti-V antibodies; (C) stain of purity analysis gel for F1-V, F1 and V proteins; (D) immunoblot of purified F1-V, F1 and V proteins using rabbit polyclonal anti-V antibodies; (E) immunoblot of purified F1-V, F1 and V proteins using rabbit polyclonal anti-F1 antibodies. Sample labels and loading amounts as follows: MWR, relative molecule weights in kDa; BRS, broad range standards (BioRad); L, crude cell lysate, 40× dilution of 118 mL total cell lysate; CL, cleared lysate, 1.6 μg; Step 1, completion of AEX stage, 2.2 μG; Step 2, completion of HlC, 1.5 μg; Lot 15A, final fill of USAMRIID lot no. 15A, 1 μg; Lot 7C, contracted material after buffer exchange and archiving at USAMRIID as lot no. 7C, 1 μg; 10−0.625, loading amounts in micrograms per lane of purified F1-V lot no. 15A; V, purified V, 1 μg; F1, purified F1 protein, 1 μg.

lowest possible laser power was used to generate spectra to prevent artificial peak formation.

For LC-ESI/MS/MS, purified protein was digested with trypsin for peptide mapping and amino acid sequencing essentially as previously described (*30*) but with the following changes. The LC MSD Trap system (Agilent Technologies Inc., Wilmington, DE) was plumbed for capillary-flow configuration, flow rate set to 20 μL/min, and 5 μL (4 pmol) of diluted sample was fractionated using a smaller Zorbax SB-C8 column (1.0 mm × 150 mm, 3.5 μm) (Agilent). Raw data were collected using an enhanced resolution mode scan rate of 5,500 (*m/z*)/s, with autoMS/MS analysis preference for all predicted F1-V tryptic peptides, entered into the method as doubly charged ions. The sample was injected four separate times while optimizing preferred ions settings and results were compiled using SpectrumMill MS Proteomics Workbench software (Agilent) to generate the total amino acid coverage shown in Figure 1. The amino terminus was also sequenced by Edman degradation using a Procise Sequencer as prescribed by the instrument and reagents vendor (Applied Biosystems).

Light Scattering Spectroscopy. Size exclusion chromatography coupled to multi-angle light scattering spectroscopy (SEC-MALS) was used to measure protein quality and to investigate quaternary structure. An 1100 LC liquid chromatography system (Agilent Technologies) was connected to a DAWN EOS multiple angle laser spectrometer and OptiLab DSP refractometer (Wyatt Technology, Santa Barbara, CA). Mobile phase buffer (DPBS, 0.01% sodium azide) was filtered on preparation (0.22 μm) and again during analysis with an inline filter (Millipore) holding a 0.1-μm VVPP Durapore membrane (Millipore), plumbed just after the instrument pump. Two SEC columns were connected in series to the heated column compartment. Several SEC packings were tested including the polymethylacrylate resin of the KW series columns (Shodex, Tokyo, Japan) and the agarose-based resin of Superose 6 HR 10/30 and Superose 12 HR 10/30 columns (Amersham). The system was equilibrated at 0.5 mL/min flow and 37 °C, and for temperature stability, the EOS and OPTILAB instruments were cooled to 10 degrees below their 37 °C set point using a model 9100 refrigerated chiller (PolyScience, Niles, IL) with 20% ethylene glycol. The entire system was equilibrated for at least 2 h before analysis. Bovine serum albumin (BSA) (Pierce) was used to normalize the detectors, applying a refractive index increment (dn/dc) value of 0.185 mL/g for all calculations. Protein samples (0.25−0.5 mg/mL in 0.4 mL injected) were filtered with 0.1-μm GHP Acrodisc13 syringe filters (Pall Corporation, East Hill, NY) immediately before analysis. Each experiment comprised a 60-min isocratic run with 30-min postrun equilibration. Molecular mass calculations were performed using ASTRA version 4.90.07 software as instructed (Wyatt Technology).

Dynamic light scattering spectroscopy provided a rapid average measure of protein size and was performed as described by the DynaPro-801 molecular sizing instrument and Dynamics software vendor (Wyatt Technology).

Vaccination, Serology, Challenges, and Statistical Calculations. Research was conducted in compliance with the Animal Welfare Act and other federal statutes and regulations relating to animals and experiments involving animals and adhered to principles stated in the *Guide for the Care and Use of Laboratory Animals*, National Research Council, 1996 (*31*). The facility where this research was conducted is fully accredited by the Association for the Assessment and Accreditation of Laboratory Animal Care International. Previously established mouse models for bubonic and pneumonic plague (*15*−*17*) were used to compare the former licensed Plague Vaccine USP and experimental vaccines containing different combinations of F1, rV, and the F1-V fusion proteins. A single dose amount near 0.6 nmol per delivered protein antigen was used essentially as described previously (*16*, *17*). Prior study had established this amount as the minimal level of administered protein to first achieve full protection against a challenge near 10^3 LD_{50} of *Y. pestis* strain CO92 (*16*), which corresponds

Table 2. Purification Summary of F1-V Fusion Protein

step	description[a]	amount F1-V (mg)[b,c]	total protein (mg)[c]	step recovery (%)	total yield (%)	fold purification[d]		purity (%)[b]
						step	total	
i	broken cells	ND	ND	ND	ND	1	1	11
ii	clarified lysate	195.1	1585.9	100	100	1.1	1.1	12
1	AEX purification	43.8	138.6	22	22	2.7	2.7	32
2	HIC purification	39.7	40.1	91	20	3.1	3.1	99
3	HIC concentration	21.7	21.9	55	11	1	1	99
4	SEC buffer exchange	19.9	20.1	92	10	1	1	99

[a] This purification summary was from 60 g of cell paste, i.e., representing 1/10 of starting material from a 20-L fermentation. Final F1-V yield as extrapolated to fermentation culture is 10 mg/L. [b] Proportional amount was measured by densitometry as described in Materials and Methods and then used to calculate amount of F1-V, step recovery, and total yield values, except for the final stage of purified F1-V in which protein concentration was measured by BCA assay and purity was evaluated by RP-HPLC. [c] Protein concentrations used to calculate total protein amounts at each stage were measured using BCA assay as described in Materials and Methods. ND, not determined. [d] Fold purifications are shown as stepwise and cumulative total calculations based on purity since F1-V has no known enzymatic activity.

to approximately 10 μg of F1 protein, 20 μg of rV protein, and 33 μg of the new non-tagged F1-V fusion. Vaccine efficacy was inferred directly from animal survival, as analyzed by life tables techniques (SAS institute Inc., Cary, NC) to estimate the mean time of survival (MST) as previously described (*16*). Relative potency was calculated as described in footnote "d" to Table 3. Studies involving the new F1-V protein in the bubonic plague model were performed similarly and analyzed using MST or by simple comparison of survival ratios, again as previously described (*16*). Briefly, trial vaccines were prepared by mixing aluminum hydroxide adjuvant Alhydrogel (1.3% Superfos, Superphos Biosector, Denmark) with protein antigen and diluted in DPBS. The volumes were calculated to achieve a final ratio of Alhydrogel to total mixture volume of 1:7 (v/v), with a final concentration of 0.2 mg elemental aluminum and desired amount of protein antigen per 0.2-mL dose. The mixture was incubated overnight at 4 °C with gentle agitation just before to use. Groups of 12 test female, 8- to 10-week-old outbred Swiss Webster Hsd:ND4 mice (Harlan Sprague Dawley, Indianapolis, IN) were administered a single dose by subcutaneous (SC) injection at a single site on the back of each animal on Day 0. Control animals received vaccine preparation with only DPBS and Alhydrogel. Blood was collected at day 35, or as otherwise indicated, and antibody titers were measured by ELISA as previously described (*17*). On Day 42, each of the vaccinated and control animals were administered a single SC injection of *Y. pestis* strain CO92 at various LD_{50} levels as indicated. Mice were observed daily to 28 days post-challenge (Day 70), at which time the survivors were anesthetized and exsanguinated by cardiac puncture.

The same basic protocol was used to study protection by the purified F1-V candidate vaccine in a mouse model for pneumonic plague by wild-type and non-encapsulated challenge strains except for the following changes: (1) candidate vaccines contained purified F1-V fusion protein at 30 μg per single dose; (2) control groups comprised five or six animals; (3) on day 51, each of the vaccinated and control animals were exposed by nose-only aerosol chamber to *Y. pestis* CO92 or *Y. pestis* CO12 at LD_{50} levels, as indicated in Table 6.

For ELISAs, serum from each animal was assayed in triplicate to measure the endpoint titer of every mouse. To generate data of high confidence, instrument readings were averaged for each step of the dilution series of three identical loadings per serum, background levels were subtracted, and then the endpoint titer was assigned as the numerical reciprocal of the highest dilution having $OD_{405} > 0.1$. Finally, an aggregate endpoint titer for all animals in each test group was calculated as the geometric mean with geometric standard error (log_{10}) calculated using an Excel spreadsheet (Microsoft, Richmond, WA).

Statistical calculations were performed using Systat Software (Point Richmond, CA) and SAS software (Cary, NC). Comparison of survival rates between test groups were calculated by the two-tailed Fisher's Exact method with stepdown Sidak correction for multiple comparisons, applying $p < 0.05$ as showing significant difference and $p > 0.05$ as not showing significant difference. Mean survival times (MST), a more rigorous measure of vaccine potency inclusive of data for animal survival as well as animal death, were derived using the Kaplan-Meier survival analysis (SAS) to calculate aggregate survival curves. Log rank tests were used to compare survival curves with 95% confidence levels. Probit analysis was used to calculate LD_{50} and PD_{50}.

Results

Selecting the Expression Strain. We redesigned the expression vector to eliminate unwanted amino acids while retaining the F1 and V regions previously demonstrated to elicit protective immunity (*16*, *17*, *19*). Using two sets of PCR fragments and an in-frame *Eco*R I union between the two genes, an improved *caf1-EcoRI-lcrV* gene fusion was situated behind the T7 promoter and *lac* operator of pET-24a and followed the by T7 terminator region. This removed the T7 gene 10 immunosorbant tag of the recipient vector altogether and displaced the C-terminal His-tag outside the translation reading frame, while eliminating a *caf1* leader sequence and correcting two *lcrV* point mutations from the prior construct (*17*), as confirmed by DNA sequencing. Evidence from SDS−PAGE gels and immunoblots (Figures 2 and 3) largely confirmed that the purified protein was as predicted from the 1437 base-pair gene fusion (GenBank accession no. AY924380) coding for a putative translation product of 478 amino acids and 53,193 calculated mass. However, subsequent investigation showed that the N-terminal Met was not present, leaving the penultimate coded amino acid, Ala, at the N-terminus (Figures 1, 4, and 5, and discussed below). Two other expression strain systems were constructed and tested for possible scaled-up production of F1-V, including *E. coli* HMS 174 (DE3)/pLysS, because of its multiple protease mutations and tighter T7 polymerase regulation, and the yeast strain *P. pastoris,* because of its prior success in high-density fermentation and production of botulinum neurotoxin type A binding domain (*26*). As shown, the *E. coli* HMS strain produced minor contaminants visible as multiply degraded forms of V (Figure 2, lane 4, panel B), and the

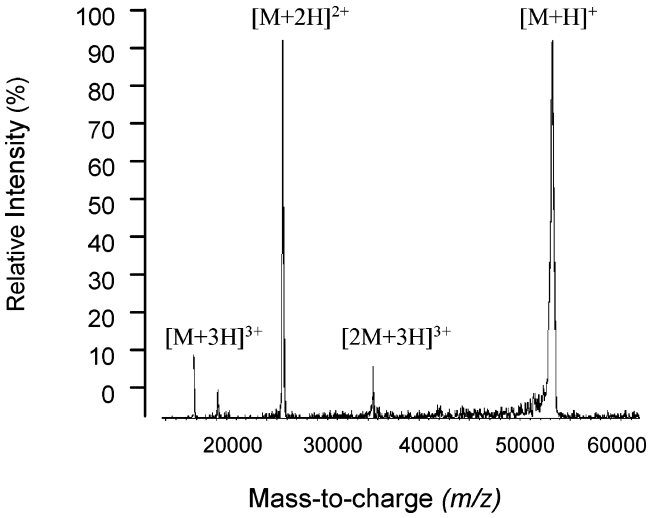

Figure 4. MALDI-TOF-MS of F1-V for whole protein mass. A representative MALDI-TOF mass spectrum for purified F1-V protein is shown with prominent ions labeled as follows: $[M + H]^+$, singly charged ion; $[M + 2H]^{2+}$, doubly charged ion; $[M + 3H]^{3+}$, triply charged ion; $[2M + 3H]^{3+}$, triply charged ion of F1-V dimer. These data reveal a molecular ion of *m/z* 53,034, concordant with the predicted mass of des-Met F1-V.

P. pastoris strain removed all detectable regions of F1 and a portion of V from the fusion protein (Figure 2, lane 6, panels A and B). In contrast, the *E. coli* strain BL21 (DE3) produced a single, clean protein band reacting to both anti-F1 and anti-V antibodies and having the expected relative molecular weight of 53 kD for F1-V protein (Figure 2, lanes 1 and 5). From these results, we concluded that the pET-24a expression system in BL21 (DE3) was superior to both alternative F1-V expression systems. Later testing confirmed that the banked research and development production strain BLR (DE3)/pPW731 produced equally clean F1-V with equivalent fermentation and induction kinetics.

Optimizing Cell Growth and Protein Induction. Trials were performed to optimize growth medium and IPTG induction of protein expression. Defined (minimal) media and various complex media comprising Super Broth and Terrific Broth were tested. Considering a risk of contamination by bovine spongiform encephalopathy (BSE) (*32*), complex growth media containing soy peptones instead of tryptone as sources of peptides, amino acids, and vitamins were tested for fermentation. The peptones were either highly reduced in animal product content (premixed medium hydrolyzed with gastric enzymes) or absolutely free of animal products (soy peptone hydrolyzed with recombinant enzymes). All tested animal-product-free complex media supported growth comparable to that provided by conventional formulations of Super Broth and Terrific Broth. Minimal expression medium with glucose as carbon source produced lower levels of growth. Because of difficulties in handling finely powdered peptones, premixed animal-product-free Terrific Broth was selected as standard medium and used along with a glycerol carbon source feed during late-stage fermentation. This medium with appropriate antibiotics supported growth to 33−35 OD_{550} in the fermentor. Conditions for inducing F1-V protein expression were then explored with regard to timing and IPTG concentration. Induction at 1.5 OD_{550} during log phase did not inhibit further growth when IPTG was added at levels between 0.4 and 1 mM. A protein of 53 kDa M_r was the major protein in whole cell lysates and accounted for 10−20% of total protein separated in SDS−PAGE gels, depending on fermentation (Figure 3, lane 2). Immunoblots developed with anti-F1 and anti-V antibodies confirmed that this same major band at 53 kDa M_r contained both F1 and V protein structures and was therefore surmised to be F1-V (Figure 3). Essentially equivalent expression of F1-V in minimal and complex media was observed by SDS−PAGE. A BL21 (DE3)/pET-24a control strain without the F1-V coding sequence did not produce immunoreactive proteins near 53 kDa M_r. These studies also revealed that the BL21 (DE3)/pPW731 expression system was somewhat leaky as F1-V was detected in the absence of induction (not shown).

Developing and Optimizing the Purification Process. A suitable method for breaking cells, harvesting crude product, and purifying F1-V by liquid chromatography, including final concentration and buffer exchange, was developed empirically through iterative application and modification of common laboratory procedures for protein purification. Several common protein manipulation procedures were found to be unsuitable for handling F1-V protein. The final process derived from our pilot purification method (lysis/AEX/SEC) used for scouting F1-V production strains. That procedure used commercial detergents (Y-PER and B-PER, Pierce) to effectively lyse cells and dissolve insoluble proteins but was judged not to be suitable for recommendation as part of a baseline method from which to develop a process for good manufacturing practice (GMP). Detergents of proprietary composition would have necessitated additional controls as residual contaminants. Because electron microscopy revealed the presence of inclusion bodies in the previous BL21 (DE3)/pET-19b-His_{10}-F1-V expression strain (Heath, D., unpublished results), we first tried to harvest F1-V protein by conventional collection and wash techniques for inclusion bodies (*33*). However, poor yields on scale-up using these procedures showed that F1-V was lost during consecutive centrifugations, suspensions, and washes. Further testing showed that approximately 75% of the total F1-V was soluble after conventional treatment with lysozyme and hypertonic buffer plus sonication. However, insoluble protein began to accumulate at cold temperature even by 24 h. Mechanical disintegration of cells in alkaline buffer, without use of lysozyme or sucrose, provided equivalent dissolution and extended solubility of F1-V on cold storage. On scale-up, more than 80% of the total F1-V protein was observed in soluble form simply after sequential microfluidization and sonication in alkaline buffer. In an effort to increase the availability of F1-V for subsequent purification, we tested chaotropic agents to denature all proteins and found that 6 M urea sufficiently increased the yield and stability of F1-V in cleared lysate.

Differential solubility by ammonium sulfate precipitation was tested for initial harvest and early stage purification, both with and without urea, but produced poor recoveries. Very little F1-V was recoverable after storing the ammonium sulfate pellet material for any length of time tested. Because of this, we omitted ammonium sulfate precipitation for use in early fractionation or as a hold step but continued to test it during all other stages for simple protein collection and buffer exchange. However, the best stepwise yields by precipitation did not exceed 50%. Ultrafiltration presented equally high losses, whether using Amicon CH2 concentrator with spiral wound cartridge (S1Y30, Millipore) or a Labscale tangential flow filtration Pellicon XL (Millipore). Because protein recoveries were often lower on larger-scale trials, we eliminated salting out procedures altogether and used filtration only where necessary in

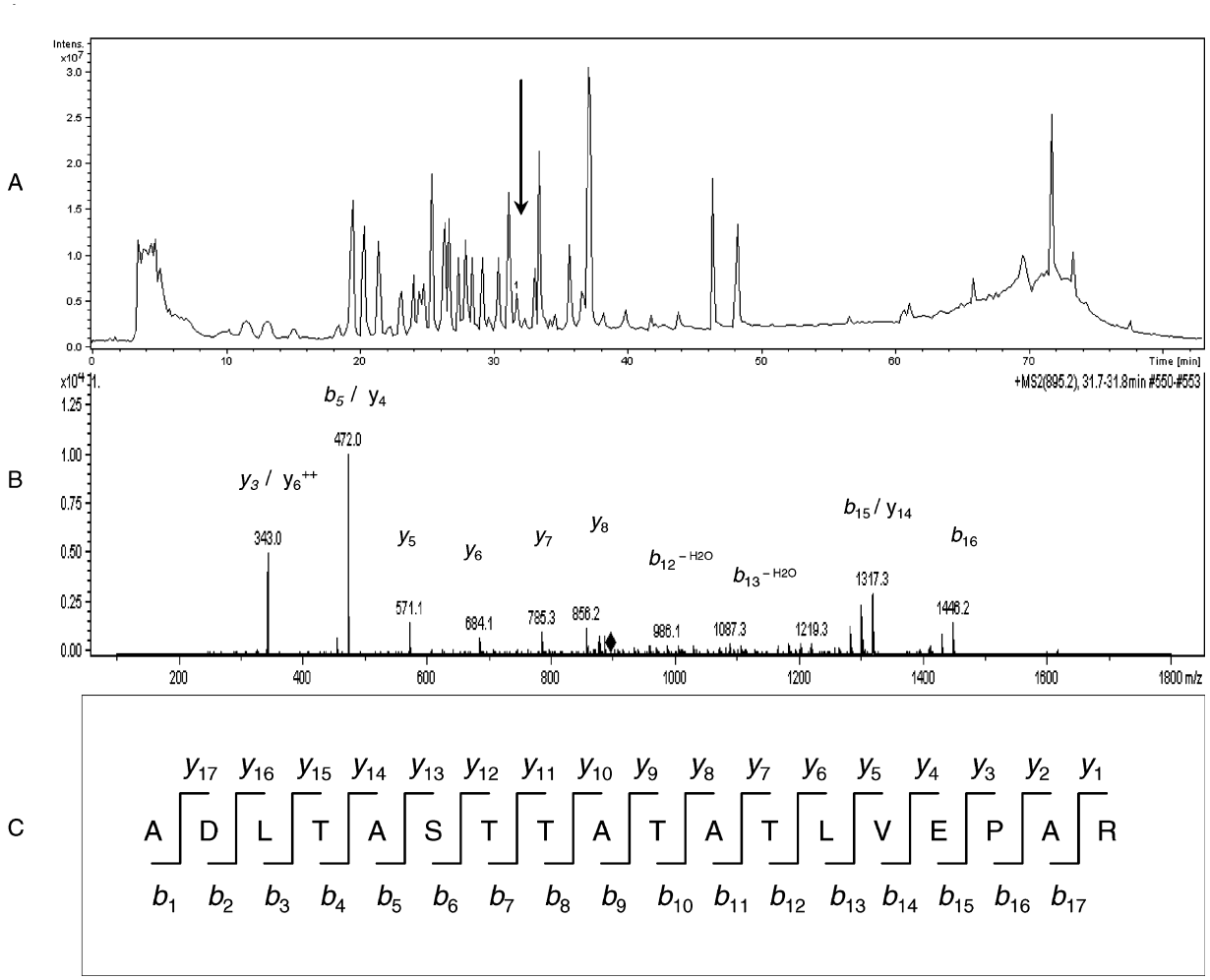

Figure 5. LC-ESI/MS/MS of F1-V for amino acid sequence. Representative results for purified F1-V are shown: (A) RP-HPLC tryptic map. Arrow indicates elution position of the amino-terminal tryptic fragment selected as primary peptide ion for fragmentation and subsequent analysis. (B) MS/MS spectrum of the indicated primary ion, with original position at *m/z* 895.2 marked by a diamond, and most intense observed *y* and *b* series ions labeled. (C) Amino acid sequence concordant with masses of observed *y* and *b* series ions. Twenty observed ions directly verified this sequence as the des-Met N-terminal peptide ion of the F1-V product.

developing the final process. We later determined these losses to be related to a tendency for F1-V protein to aggregate under conditions of high salt or cold temperature. In addition, we observed that buffers more acidic than pH 6 tended to reduce F1-V solubility, as did rapid changes in pH or repeated freeze/thaw treatments. Neither gentle heating at 37 °C nor resuspension with 0.1% Tween-80 or 0.1% octyl glucoside noticeably reversed the insolubility of visible F1-V aggregates. Sodium chloride decreased F1-V solubility on approaching 1 M or less, depending on the nature of prior treatment of F1-V. Alternatively, a large portion of F1-V aggregates returned to solution by suspension in high pH buffer, including ethanolamine at pH 10. Consequently, a buffer base of 20 mM ethanolamine adjusted to pH 9.5 was chosen for chromatography and ultimately used throughout most of the final process.

Selection of Chromatography Chemistries. Several resin chemistries, buffers, column formats, and running conditions were tested for purification of F1-V by sequential stages of liquid chromatography. Immunosorbent chromatography with polyclonal antibodies against F1 and V was tested but later eliminated from further testing due to the lack of sufficient quantities of monoclonal antibodies and likely future costs associated with qualifying and replacing antibody reagent stocks. Of the cation exchange (CEX) resins tested (SP Sepharose, CM Sepharose, and DEAE Sepharose), none selectively bound F1-V under several different pH conditions tested. Heparin Sepharose resin was also tested as V protein contains amino acid sequences ($KX_{12}KR$, KX_7KR, KKX_4K) somewhat resembling the dual clusters of basic amino acids present in heparin-binding domains (*34*), but F1-V did not bind under various conditions tested including near neutral pH. Similarly, hydroxyapatite resin (Rainin, Columbus, OH) with potassium phosphate buffer at pH 7.2 or higher was not selective for F1-V. Of AEX trial resins tested, the strong anion-exchange resin Q selectively bound and eluted F1-V very well in research-scale (Resource Q) and process-scale (Source 15Q) formats and was therefore chosen as the first purification step. MacroPrep Q (BioRad), a similar AEX resin that we successfully applied for scaled-up production of the anthrax protective antigen (*35*), did not perform as well for purifying F1-V. Because the Q resin was successfully used for on-column refolding of other denatured insoluble proteins (*36*−*39*), this technique was tested and applied as the first purification step for F1-V. Step 1 conveyed a 2.7-fold purification of F1-V in the final optimized process (Table 2). Although F1-V was present the flow-through fraction, it was not effectively captured by a second passage over the column. Apparently, much of this F1-V was in a form that did not penetrate gradient SDS−PAGE gels on analysis (data not shown). For HIC, the

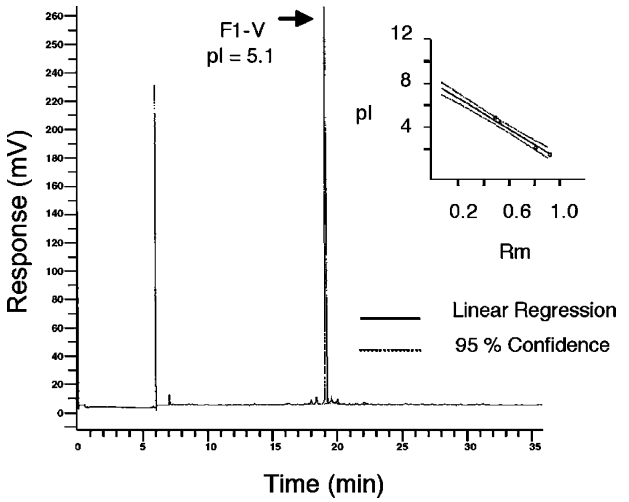

Figure 6. CIEF of F1-V for isoelectric point. Inset: standard curve showing linear regression and 95% confidence interval.

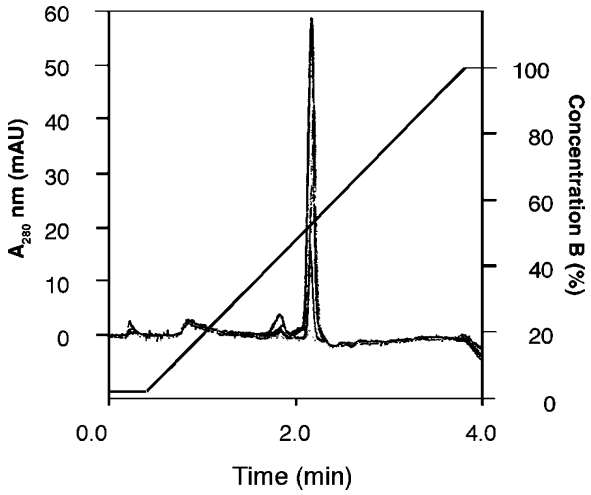

Figure 7. RP-HPLC of F1-V for protein purity. Absorbance vs elution time plots are overlaid for five USAMRIID purification lots and one contracted lot of F1-V protein.

POROS 20 PE resin initially showed optimal performance in small- and large-scale purifications but was later abandoned as it is no longer commercially available (Applied Biosystems). As an alternative resin, butyl Sepharose FF and Octyl Sepharose FF both performed well on a small scale. However, on scale-up to 1-L bed volume, Octyl Sepharose bound F1-V too tightly for efficient elution and recovery under the buffer conditions and temperatures tested, including column cooling to 18 °C. Sepharose CL-4B (Amersham) was tested as a weak HIC resin and eventually applied in a different purification scheme that did not involve protein denaturation (Powell, B., unpublished data). In contrast, Butyl Sepharose performed well on scale-up to 1-L bed volume and was therefore selected for the second chromatographic step of the optimized process. At 91% stepwise recovery and 3.1-fold stepwise purification, this method yielded F1-V at 99% purity as applied in Step 2 of the process (Table 2). However, concentrating F1-V beyond this stage was problematic as a result of the aggregative nature of F1-V. Diafiltration or centrifugal collection of precipitated protein each resulted in high losses of F1-V, so column capture and buffer change were tested using HIC and AEX. Ammonium acetate provided better binding and total recovery than did ammonium sulfate, sodium sulfate, or sodium chloride and resulted in 55% stepwise recovery of F1-V at this stage of the process (Table 2). A similar approach using AEX was also successful on a small scale but required too large a sample dilution to be practical for large scale. Size exclusion chromatography (SEC) was chosen for final cleaning and changes into the holding buffer, due again to known losses caused by salting-out or by membrane filtration (see above). This gave 92% stepwise recovery (Table 2). Of several syringe filters tested for filtration before final storage, the Millex-GV syringe filter (Millipore) containing a 0.22-μm Durapore membrane permitted up to 96% recovery of pure F1-V. When fractions were assayed during purification, the relative amount of soluble F1-V in the sample lanes of the stained gels appeared not to concur with predicted low yields from chromatographic traces of absorbance at 280 nm (A_{280}). Spectroscopic measurements of purified F1-V confirmed that it had an abnormally low A_{280} compared to other proteins. Thus, A_{280} was judged not to be a dependable indicator to monitor F1-V purification, and instead A_{215}, A_{260}, and A_{280} were all recorded and compared during chromatographic procedures. Because of low absorptivity, A_{280} was also deemed to be less useful for measurements of final purity and concentration (see below).

Biophysical Characterization. The identity of purified F1-V protein as being similar to the intended gene product (Figure 1) was supported throughout discovery and process development by observing relative sizes of protein in SDS−PAGE gels and immunoblots (Figures 2 and 3). In all cases, a prominent band was observed near 53 kDa M_r that bound anti-F1- and anti-V antibodies. Analysis of the N-terminus by Edman degradation indicated an amino acid sequence of ADLTASTTAT, which differed from the predicted translation product by missing the putative N-terminal Met, in agreement with its removal during expression in *E. coli*. This conclusion was first supported by MALDI-TOF-MS analysis of whole protein mass in which a prominent molecular ion was observed at *m/z* 53,034 (Figure 4). This value was within 27 Da of the calculated mass for a putative F1-V translation product missing its N-terminal Met (53,061), representing a mass difference of 0.05%, less than instrument error or the smallest amino acid (Gly at 58 Da). Alternatively, the measured value differed by 159 Da from a putative whole F1-V translation product of 53,193 Da. Although mass accuracy was slightly affected by the NaCl content through peak broadening, as was apparent for the primary ion $[M + H]^+$ (Figure 4), this effect cannot account for the large observed difference. Protein identity and primary structure were then verified by liquid chromatography coupled to electrospray ionization tandem mass spectrometry (LC-ESI/MS/MS), which detected 89% of the amino acid sequence coded by the *caf1-EcoRI-lcrV* gene fusion product (Figures 1 and 5). This percent coverage was compiled from four separate analyses at various instrument settings, using custom protein databases containing either the whole or the des-Met version of F1-V amino acid sequence, and in no case was an N-terminal peptide ion containing a terminal Met observed. In agreement with this, a doubly charged tryptic peptide ion of 895.2 *m/z* (1788.4 Da) was observed at the amino terminus without the coded N-terminal Met (Figure 5). This ion had a peptide score of 15.63 and a score peak intensity of 90.6%, which exceeded the default cutoff values of 9% and 70%, respectively, for automated validated identification. To confirm this beyond reasonable doubt, *y* and *b* series ions were inspected manually and 20 observed ions directly verified the N-terminal peptide with des-Met sequence (Figure 5C). Similar

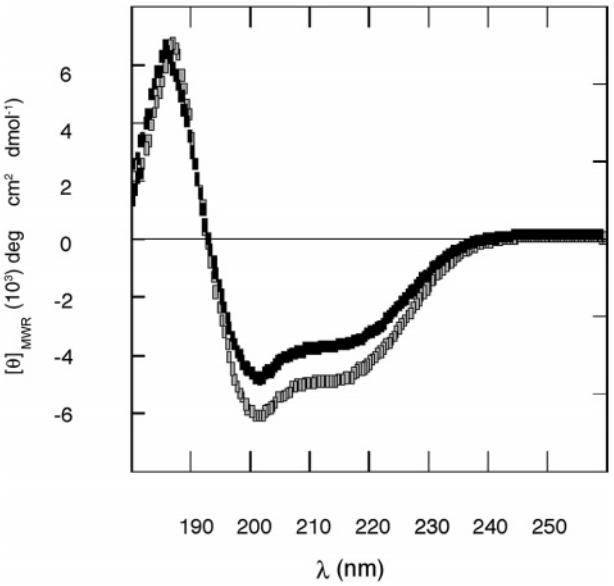

Figure 8. CD spectroscopy of F1-V for secondary structure. Near-UV CD spectra are overlaid for two different lots of F1-V: (dark shaded data points) F1-V lot no. 1 produced by an abbreviated process comprising steps 1 and 4; (light shaded data points) F1-V lot no. 5 produced by the optimized process described in Materials and Methods. Differences in amplitude are due to nonidentical sample concentrations.

inspection of MS/MS data also confirmed the intended dipeptide linker between F1 and V regions and much of the total amino acid sequence (Figure 1). An isoelectric point of 5.1 was measured (Figure 6) by capillary isoelectric focusing (CIEF), in agreement with the calculated value of 5.2 for F1-V. In total, these data provided convincing evidence that the purified protein concurred with a putative F1-V fusion protein of primary structure and unit mass of 53,061 Da, concordant with 477 of the 478 coded amino acids and having N-terminus at the second coded amino acid, alanine. These results also showed that purified F1-V contained no large truncation, proteolysis, or other detected posttranslational amino acid modification.

Purity and concentration were routinely measured during purification by stained SDS−PAGE gels and corresponding immunoblots (Figure 3). All F1-V preparations contained some detectable amount of breakdown product. However, lower bands observed near 23 and 38 kDa M_r on immunoblots of final preparations were not detected by Coomassie stain (Figure 3, lane 7, panels A and B) and therefore were judged to be F1-V degradation products of minute concentration. The apparent high specificity of these antibodies, as evidenced by single bands on immunoblots of unpurified protein preparations (Figure 2 and Figure 3A vs 3B), disfavors the alternative possibility that these immunoreactive bands might represent contaminating proteins unrelated to F1 or V. To further reduce doubt about possible nonspecificity in detection by cocktail, immunoblots were performed on F1-V, rV and F1 proteins separately with each of these same antibodies (Figure 3, panels D and E). Stepwise and total yields derived from gel densitometry are summarized in Table 2. Purity of final F1-V preparations was also evaluated by reversed-phase high-pressure liquid chromatography (RP-HPLC), after developing a suitable mobile phase eluant. The fusion protein precipitated from solution in standard RP-HPLC low pH mobile phase buffer, so alkaline RP-HPLC using sodium hydroxide as pairing ion (*35*) was tested. Because this also caused precipitates, hydrochloric acid was tested as a gentler pairing ion compared with the conventional trifluoroacetic acid. F1-V was more soluble in this mobile phase. Five purified lots of F1-V were compared and each contained a primary peak at 2.2 min (22 ± 0.06 mL) with a minor peak representing contaminating protein (Figure 7). However, this assay was not used to measure purity because of the uncharacteristically low A_{280} of F1-V, which would bias the evaluation of integrated peak areas. In direct comparisons, the relatively high absorbance of contaminating proteins generated lower purities than were measured by gel densitometry. In contrast to UV absorbance measurements, the BCA method with extended dilution range provided consistent and representative measurements of F1-V concentration and was therefore chosen for protein concentration assays. Biological strength, i.e., potency, was inferred from tests of immunogenicity in animal studies (see below).

Secondary and tertiary structures were measured by intrinsic tryptophan fluorescence and CD spectroscopy and then compared among different production lots to measure consistency with respect to protein folding. A characteristic double minima CD spectrum was observed among different tested lots of F1-V protein. The observation of minima near 205 and 215 nm indicated substantial coil and α content together with comparably less β structure (Figure 8). Theoretical structures were predicted for the F1-V amino acid sequence and a consensus among eight theoretical structures (*28*) assigned high random coil (46%) and α-helix (34%) content but notably less extended strand (16%) and ambiguous (4%) states (Figure 9). Thus, the predicted and measured secondary structures were in agreement. Interestingly, much of the extended strand and random coil mapped within the F1 portion, while nearly all of the α-helix mapped within the V portion of the total sequence (Figure 9). Regarding tertiary structure, similar spectra comprising a broad peak at 360 nm were observed among four separate production lots including both the early and final purification processes (Figure 10). The consistency of the observed secondary and tertiary structures between purification lots concur with the notion that F1-V folds stably and consistently by this general purification process.

Bioburden in the form of nucleic acid and endotoxin were tested in five separate lots and observed to range from 3 to 13 ng/mg and 25 to 379 EU/mg, respectively. The absence of a trend in the CD spectra toward high positive rotation peak at 280 nm also indicated no measured nucleic acid in the samples. These contaminant levels were considered to be sufficiently low for use in animal studies, and results from subsequent use in several experiments confirmed this prediction. On occasion, however, endotoxin levels were higher for an undetermined reason. An effort to remove endotoxin from early preparations of F1-V using Detoxi-gel (Pierce) resulted in recoveries less than 50%, as was previously observed for F1 production (*15*). This was not attempted again. Thereafter, column-cleaning practices were established after every use as described in Materials and Methods. The safety of F1-V was assessed in mice using an acute toxicity test and determined to produce no adverse effects, as will be reported separately (Andrews, G. and Powell, B., unpublished results).

Variation in protein quality first became evident during process optimization and was later measured while characterizing quaternary F1-V structure. This variability was determined to be a consequence of protein self-association. Multimeric F1-V was first noticed as dimers by SDS−PAGE and immunoblot (Figure 2, lane

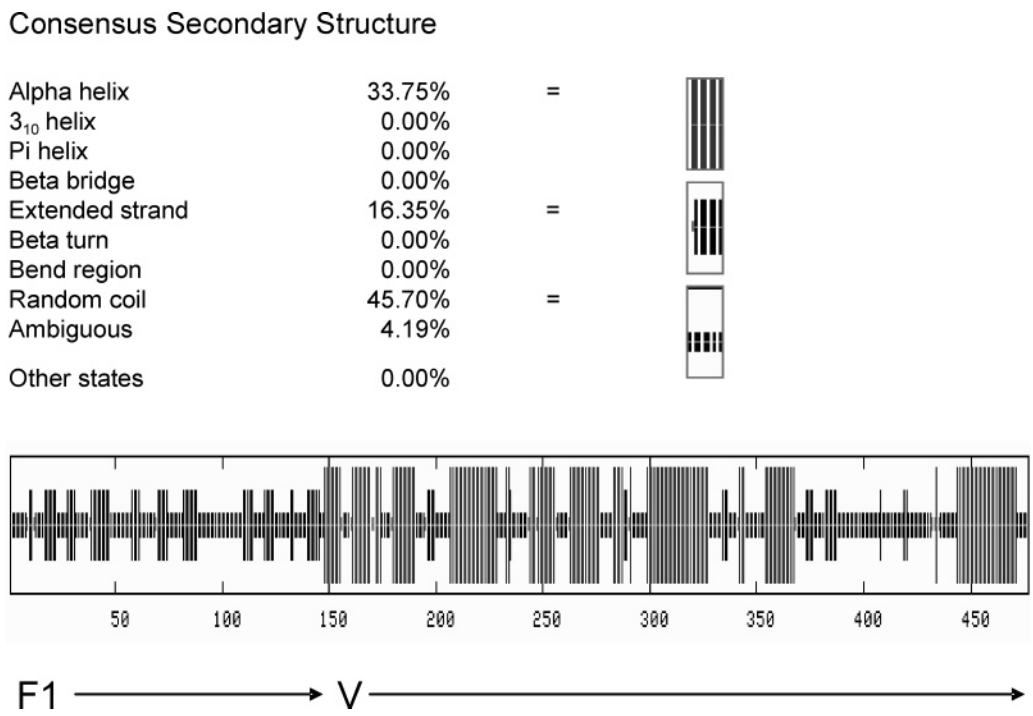

Figure 9. Predicted secondary structure of F1-V fusion protein. A consensus secondary structure derived from eight separate predictions is shown, calculated as described in Materials and Methods: (top) overall percentages by structural subgroup; (middle) per residue prediction mapped onto amino acid sequence of the expressed des-Met fusion protein; (bottom) arrows depict the extent of each subunit in the protein fusion (arrowhead = carboxyl end): F1, AA 2−150; and V, AA 153−148. Key: tall bar, α-helix; medium bar, extended strand; short bar, random coil.

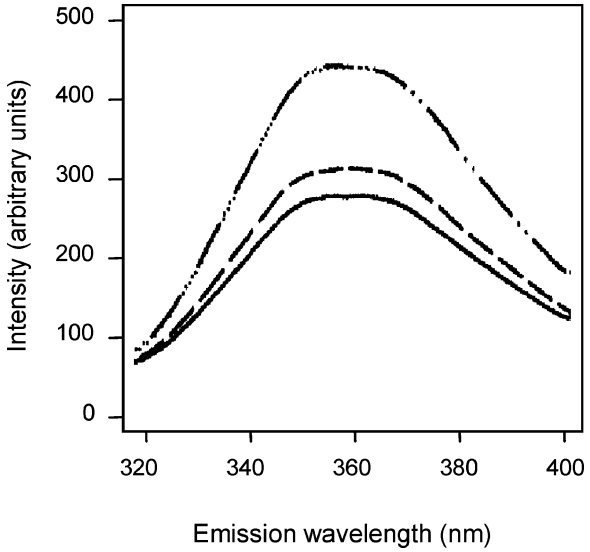

Figure 10. Intrinsic fluorescence spectroscopy of F1-V for tertiary structure. Tryptophan emission spectra in the near-UV region are overlaid for four different purification lots of F1-V. Differences in amplitude are due to nonidentical sample concentrations.

5; Figure 3, lot 7C), and was particularly evident when the sample was insufficiently heated in fresh loading dye. SEC chromatograms of purified F1-V showed a broad central peak with approximately three additional shoulder peaks for all lots. The amplitude of these peaks varied according to conditions such as the length of holding time at 4 °C or number of prior freeze/thaw treatments. The central peak of greatest concentration appeared between 200 and 500 kDa in relative size, while some amount of F1-V always exceeded the column void volume. Further testing with other SEC columns indicated that pure F1-V contained molecular structures that ranged from the expected monomeric form of 53 kDa to sizes greater than were measurable by standard curves constructed with any commercially available column ($\sim 10^6$). Attempts to measure F1-V size by dynamic light scattering spectroscopy were inconclusive because existing software algorithms cannot resolve data of such high polydispersity, i.e., nonagreement between number-averaged and weight-averaged masses. This impasse was due to instrument design, which measured a single angle of scattered light, and to sample complexity, as F1-V apparently contained a large number of different molecular sizes. Therefore, we measured the quaternary structure of F1-V by multi-angle light scattering spectroscopy in-line after fractionating the sample with size exclusion chromatography (SEC-MALS). This method measures the averaged absolute masses of molecules as they fractionate through SEC (Figure 11). A single protein standard, BSA, which is used conventionally as an isotropic scattering reference to calibrate the instrument detectors, clearly resolved into molecular forms of absolute mass corresponding to monomer (66 kDa), dimer (132 kDa), and detectable trimer (198 kDa). Purified V protein separated into monomer (38 kDa) and dimer (76 kDa) forms with very little higher order structures detected. Pure F1 protein, of 15,694 Da in monomeric mass, appeared as a wide ranging distribution of forms, with maximum at 6×10^7 Da, but the highest concentration centered at an averaged mass near 3×10^6. Polydispersity was evident for F1 protein as the disparity in alignment between chromatographic traces for scattered light at 90° (Figure 11, dashed line) and concentration by differential refractometry (Figure 11, thin solid line). In comparison, F1-V of 53,061 Da monomeric mass separated into a wider distribution with greater polydispersity but smaller maximum size (10^7) and smaller bulk molecular form at an averaged mass of 212,000 (Figure 11). Thus, most of pure F1 protein aggregated into a molecule of mass equivalent to a 200-mer, whereas most of F1-V associated into a molecule of mass equivalent to a tetramer.

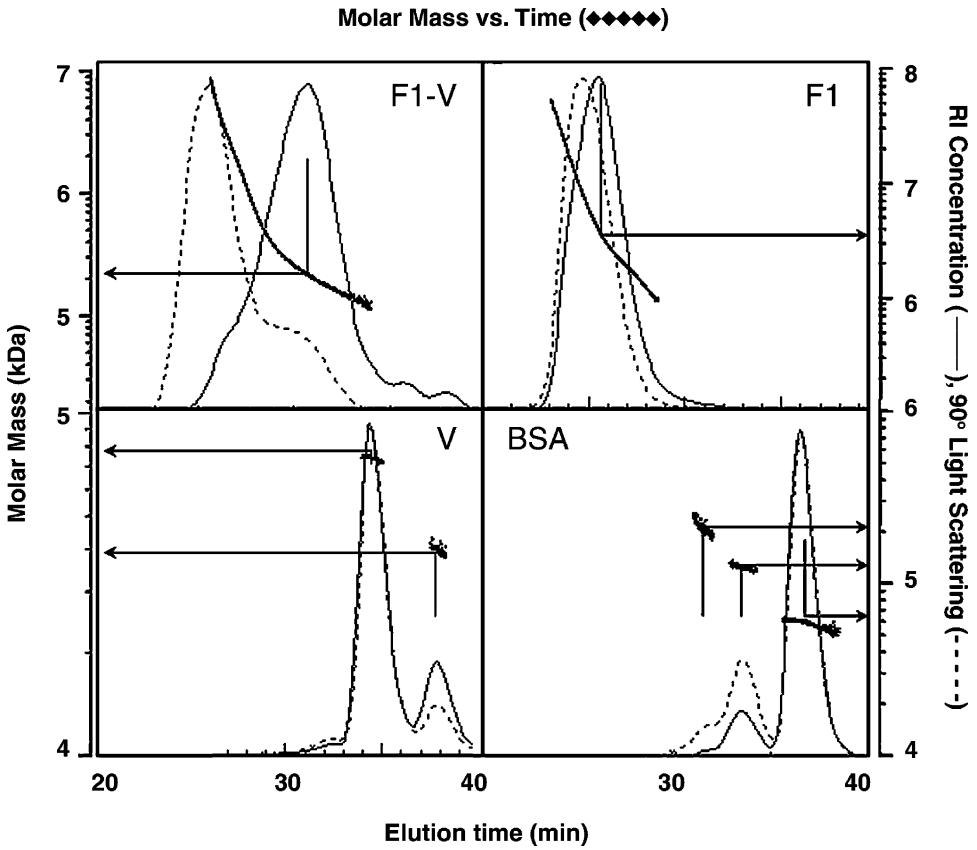

Figure 11. SEC-MALS of F1-V for quaternary structure. Typical molar mass vs elution time plots are shown separately for purified F1-V, F1, V, and BSA proteins with traces for concentration by refractive index (thin line), scattered light measured by one of 18 detectors (dashed line), and molar mass (thick line) calculated by instrument software. Data were collected and compared between two separate 90-min runs as described in Materials and Methods. Perpendicular lines from peaks of highest concentration and their associated arrows to scaled axes provide visual aide for estimating molar mass. Precise values at molar mass vs elution slices spanning the indicated peaks provided by instrument software are given in Results.

Protective Efficacy and Immunogenicity. Mean survival times (MST), a statistical measure of vaccine effectiveness that simultaneously accounts for total survivorship as well as aggregate death rates, indicated that test vaccines comprising the original His_{10}-F1-V fusion protein antigen, an F1 + rV cocktail, or rV alone each provided very good protection against lethal subcutaneous challenge. In contrast, MST values indicated that relatively poor protection was provided by test vaccines of either F1 alone or the former licensed Plague Vaccine USP (Table 3). Interestingly, protective efficacy provided by the fusion protein appeared to be better than that of the F1 + rV cocktail vaccine up to and including a high challenge dose of 10^8 LD_{50} (Table 3). A statistical comparison of these measurements called relative potency was used to test these apparent relationships as follows. First, data across multiple exposure levels for each vaccine were used to compute the protective dose providing 50% protection (PD_{50}) at a theoretical equivalent exposure, and PD_{50} values were observed to convey the same trend (Table 3). The PD_{50} values were then used to directly compare test vaccines, after normalization to equipotent challenge doses and statistical computation of relative potencies with upper and lower error limits of 95% confidence. Hence, the relative increase in effectiveness of each vaccine in comparison to the USP vaccine was observed to be 5,750-fold for the original fusion protein, 1,150-fold for the cocktail vaccine, and 500-fold for the rV antigen alone (Table 3). Curiously, the F1 vaccine was 17 times less effective than the USP vaccine under these conditions. One explanation for this may be the variable amount and altered quality of F1 protein in the USP vaccine (see Table 3, footnote a). By statistical cross comparisons that account for the error limits inherent in each value of relative potency, the fusion protein was at least 1.86 times more potent than vaccination by rV alone, and at least 1.95 times more potent than the F1 + rV cocktail vaccine in this established mouse model for bubonic plague caused by the wild-type strain of *Y. pestis*. In evaluating MST for mice vaccinated with partially purified antigen preparations from various expression strains, the F1-V fusion protein and cocktail of individually purified proteins generally provided high protection against challenge levels up to 10^8 LD_{50} (Table 5). There was no statistically significant difference in protection observed between the prior and redesigned F1-V fusions (groups 2 vs 3, Table 5 and footnote b). In contrast, the fusion protein isolated from *P. pastoris* did not protect well at any challenge level tested, and this difference was significant, having $p < 0.05$ (groups 2 vs 4). Review of protein quality from this preparation (Figure 2) indicated that all of F1 and part of V were absent in this preparation, presumably removed by an N-terminal exopeptidase, implicating the importance of the lost protein regions for protective immunity against a virulent wild-type strain. By molar amount of each antigenic polypeptide injected, the cocktail contained nearly twice as many molecules with F1 structure as were present in the fusion protein formulations (Table 5). By this analysis, no statistical difference in protection was observed between preparations containing either fusion protein antigen versus the F1 + rV cocktail. However, this test differed from the prior study (Table 3) by using a 2:1 molar ratio of F1 to V, and in

Table 3. Comparison of F1-V Fusion Protein Antigen to Plague Vaccine USP for Protective Efficacy in a Mouse Model of Bubonic Plague

vaccine[a] antigen	MST[b] and [SE] per LD_{50} exposure[c]						PD_{50}[d] {95% CL}	relative potency[e]
	10^2	10^3	10^4	10^7	10^8	10^9		
control	3.87 [0.27]	- -	- -	- -	- -	- -	NA	NA
USP	26.13 [2.20]	24.13 [2.08]	24.80 [2.04]	- -	- -	- -	4.75 {-,-}	1
F1	28.07 [- -]	26.93 [1.98]	14.47 [2.51]	- -	- -	- -	3.51 {3.15, 4.01}	0.06
rV	- -	- -	- -	21.27 [3.18]	12.87 [3.14]	4.67 [1.02]	7.45 {6.89, 7.83}	500
F1 + rV	- -	- -	- -	25.07 [2.56]	11.79 [2.54]	11.21 [3.19]	7.81 {-,-}	1150
His_{10}-F1-V	- -	- -	- -	29.00 [0.00]	20.20 [3.16]	13.46 [3.66]	8.51 {8.10, 9.16}	5750

[a] Protein sources, vaccine preparation, challenge by SC administration, observations, and calculations are as described in Materials and Methods. Protein amounts per single dose were all approximately 0.6 nmol except for the Plague Vaccine USP (USP), which has a variable amount of formaldehyde cross-linked F1, observed to range from 5 to >50 μg per 0.2-mL dose among tested lots (Andrews, G., unpublished data), and contains no detected V protein, as established previously (*15*, *17*) and confirmed herein with Table 4. Control, Alhydrogel depot vehicle in PBS without protein antigen. NA, not applicable. "- -", not tested. [b] MST, mean survival time in days averaged over all animals per group. SE, standard error in ± days, is shown in [ ]. Statistical tests for trend in death rate with increasing challenge dose used during Probit analysis were as follows: USP, $p = 0.37$, did not achieve a good dose response; F1, $p < 0.0001$; rV, $p < 0.0001$; F1 + rV, $p = 0.0005$; F1-V, $p = 0.0003$. [c] LD_{50}, half lethal dose multiple used to expose animals to *Y. pestis* strain CO92 by subcutaneous (SC) delivery. One LD_{50} of CO92 for this strain of mouse is 1.9 colony forming units (CFU). "- -", not tested. [d] PD_{50}, equipotent challenge dose level producing 50% mortality, presented in log base 10, are shown. 95% lower and upper confidence limits are given in { }. "-,-", lack of fit to the Probit regression or not calculated as a result of 100% survival. [e] Relative vaccine potency was calculated using the ratio of the PD_{50} value of each vaccine group to the PD_{50} of USP. Minimum relative potency was defined as the ratio of the lower 95% confidence limit of a PD_{50} for one vaccine to the upper 95% confidence limit of a PD_{50} for the second vaccine.

having fewer test animals per group, and therefore cannot be directly compared in this regard.

In testing efficacy in the mouse model for pneumonic plague, animals vaccinated with a single dose of the highly purified new F1-V antigen were also very well protected against lethal challenge by *Y. pestis* strains with and without capsule (Table 6). Full or very high protection was observed from aerosol exposure to 100 LD_{50} of wild-type *Y. pestis* strain CO92 or 10 LD_{50} of non-encapsulated *Y. pestis* strain C12. Very high protection was provided even at the excessive aerosol exposures of 600 LD_{50} CO92 or 100 LD_{50} C12, as was previously demonstrated for the histidine-tagged fusion protein (*17*). No differences of statistical significance were observed among vaccine groups except in relation to the negative controls (Table 6, footnote c).

In each of these experiments, all surviving mice developed high circulating antibody titers against F1 and V proteins as immunized, whereas no specific immunity was detected in animals that received mock vaccine without antigen (experiments represented by Tables 3−6). Animals immunized with the Plague Vaccine USP developed lower anti-F1 titers than other groups receiving F1 protein and did not develop any appreciable pre-challenge antibody to V (Table 4). Although the anti-F1 titer of animals immunized with the former licensed vaccine appeared lower than that achieved by the F1 or F1-V fusion protein vaccines, comparison of the geometric means revealed that the differences were not statistically significant (Table 4 and footnote b). A similar caveat is applicable to the apparent differences in GMT observed between the anti-F1 and anti-V responses among groups receiving the corresponding F1 and V subunits or fusion proteins, and again, statistical differences in titer between these groups were not significant at 95% confidence level.

Discussion

Historical Pursuit. The search for an effective plague vaccine dates back to an outbreak in India that began in 1896 and eventually killed 13 million people (*11*, *12*). A protective formulation of heat-killed, phenolyzed *Y. pestis* broth culture was created by W. M. W. Haffkine and tested in rabbits in 1897. Its safety was tested on the inventor himself and his friends, and human efficacy was established by inoculating volunteers during a plague outbreak in a neighboring jail, before being used for field vaccination. A live attenuated vaccine was used in Madagascar from the same time period, and a subsequent version called EV76 has been in continual use against plague outbreaks there since the mid-1930s. That vaccine is not licensed for use in the United States or European Union and is now known to be less effective and more reactogenic than a killed whole cell (KWC) vaccine first developed for the U.S. Army during World War II. The "Army Plague Vaccine" was created by Karl F. Meyer from an agar-grown, formaldehyde-killed, saline suspension of virulent plague bacilli. Originally manufactured by Cutter Biologicals (license no. 8), licensure was transferred to Greer Laboratories in 1994 (no. 308) for production under the name "Plague Vaccine USP." Although superior in its time, this vaccine was difficult to produce, specified a cumbersome and variable multiple-dose vaccination schedule, was reactogenic in patients, allowed some cases of plague in vaccinated individuals, and was finally shown to be ineffective against pneumonic plague (*15*, *16*, *23*, *40*−*42*). Although the Plague Vaccine USP is currently classified by the FDA as a Category I biologic, i.e., licensed biological product determined to be safe, effective, and not misbranded (*43*), it is no longer manufactured. In addition to these KWC and live-attenuated vaccines, subunit vaccines against *Y.* pestis have also been developed, including compositions of isolated cell fractions and, most recently, recombinant proteins (*15*−*18*, *30*, *42*, *44*). Methods and regulatory oversight for the development, manufacture, testing, use, and sale of vaccines and drugs have improved considerably since discovery of the first plague vaccine. Documentation of product consistency and safety (*45*), plus efficacy in animal models of disease with well-reasoned reference to human physiology (*46*), underlie the contemporary discovery and development of medical treatments against diseases such as plague that cannot be directly tested for effectiveness in people.

Contemporary Concerns. An increasing concern for protection against aerosol exposure possibly involving non-encapsulated strains of *Y. pestis* prompted recognition in the early 1990s of the need for an effective plague vaccine to replace the existing licensed product. In the late 1990s, the U.S. Department of Defense issued advanced development objectives for new products to protect against pneumonic and bubonic forms of plague.

Table 4. Immune Titers Against F1 and V Before and After Lethal Challenge

test group[a]	GMT[b] and GSD[c]			
	F1		V	
	pre[d] [GSD]	post[d] [GSD]	pre [GSD]	post [GSD]
control	320 [1.00]	NT	320 [1.00]	NT
USP	5,284 [3.24]	28,006 [3.63]	330 [1.16]	1,170 [2.92]
F1	43,563 [3.50]	60,727 [4.28]	320 [1.00]	453 [2.01]
rV	320 [1.00]	11,763 [8.03]	10,560 [3.75]	59,280 [3.21]
F1 + rV	37,858 [2.76]	62,084 [4.32]	9,027 [3.98]	20,478 [4.07]
His_{10}-F1-V	22,463 [2.39]	60,866 [8.41]	18,962 [2.91]	41,985 [2.83]

[a] Test groups, vaccine formulation, immunization, and challenge are as described in Table 3. [b] GMT, geometric mean titers, were derived from the log titer endpoints of anti-F1 and anti-V titers as described in Materials and Methods. [c] GSD, geometric standard deviation, were also derived from the log titer endpoints as described. The error interval is equal to the GMT value multiplied and divided by its GSD. Since the GSD ranges of pre-challenge anti-F1 titers for the USP, F1, F1 + rV and His_{10}-F1-V groups all overlap, these values do not differ significantly at 95% confidence intervals. Significant statistical differences were observed for control compared to all other groups except in relation to the rV group for anti-F1 and the F1 and USP groups for anti-V. [d] Sera were collected from all animals 32 days after immunization (pre) and from surviving animals 28 days after challenge (post), for measurement as described in Materials and Methods.

Table 5. Comparison of Active Protection in a Mouse Model for Bubonic Plague by a Single Dose of Various Fused and Individual F1 and V Protein Antigens

test group[a]	vaccine antigen[b]	prod'n strain	MST[b] and [SE] per LD_{50} exposure		
			1.7×10^6	1.7×10^7	1.7×10^8
1	control	NA	3.67 [0.21]	- -	- -
2	F1-V	BL21	24.42 [3.27]	28 [0.00]	17.08 [2.98]
3	His_{10}-F1-V	BLR	26.00 [2.59]	26.30 [0.00]	20.42 [3.59]
4	F1-V	pichia	6.0 [2.03]	4.08 [0.31]	3.17 [0.34]
5	F1-V	HMS174	23.17 [3.03]	22.67 [3.27]	15.08 [3.44]
6	F1 + rV	BL21	26.00 [0.00]	20.58 [3.52]	12.33 [2.78]

[a] In this experiment, 12 animals were tested per group and the observation period was 28 days post-challenge. [b] Protein sources and production strains, vaccine preparation, challenge by SC administration, and calculations are as described in Materials and Methods. Group 1 was vaccinated with a negative control comprising Alhydrogel and PBS without antigen. Protein antigen amounts in vaccines, calculated using best unit molecular masses given in legend Figure 2 and footnotes to Tables 1 and 3, were all near 0.6 nmol delivered per single dose except for Group 6, which received 1.15 nmol F1 (18 μg) + 0.4 nmol rV (15 μg). Control and "- -" as per Table 3. [c] MST,mean survival time in days averaged over all animals per group. SE, standard error in ± days, is shown in brackets, "[]." P-values for comparisons of survival curves are as follows: $p > 0.05$ for groups 1 vs 4, 2 vs 3, 2 vs 5, 2 vs 6 and 3 vs 6; and $p < 0.05$ for groups 1 vs 2, 1 vs 3, 1 vs 5, 1 vs 6, 2 vs 4, 4 vs 5, and 4 vs 6. [d] The SC LD_{50} for CO92 is 1.9 CFU.

Toward these objectives, a concerted effort for discovering and testing alternate protective antigens and improved formulations has been underway at USAMRIID and other research institutes (*15*−*17*, *19*, *42*). The most efficacious candidate plague vaccines tested to date contain recombinant versions of the *Y. pestis* capsular protein F1 and the low calcium-inducible V antigen (*42*, *47*). Two approaches were undertaken for producing and testing a subunit vaccine containing both F1 and V. One approach involved the separate production and ad-mixing of individual F1 and V proteins, whereas the second approach used a single recombinant product comprising an F1-V fusion antigen. Candidate vaccines for both approaches have been tested and each produced apparently equivalent animal protection in parenteral and aerosol challenge by natural and non-encapsulated *Y. pestis* strains (*16*, *17*, *19*, *44*, *47*). Consequently, regulatory and business concerns including safety, product control, consistent formulation, and total manufacturing and licensing costs may be more important criteria for selecting between the single fusion substance and the two-substance cocktail of apparently equivalent efficacy. Described herein is a simple scalable process for the production of an improved F1-V fusion protein with demonstration of its very high effectiveness for protection against both bubonic and pneumonic plague.

Table 6. Active Protection by a Single Dose of the Improved F1-V Vaccine in a Mouse Model for Pneumonic Plague with Encapsulated or Non-encapsulated *Y. pestis*

treatment group	antigen[a]	challenge strain[b]	dose[b] (LD_{50})	survival[c]	TTD[d]
1	F1-V	CO92	100	12/12	- -
2	F1-V	CO92	600	11/12	3
3	F1-V	C12	10	10/12	5
4	F1-V	C12	100	11/12	6
5	control	CO92	100	0/6	3
6	control	C12	10	0/5	4

[a] Purified F1-V, vaccine preparation, administration, and challenge strains are as described in Materials and Methods. Control, negative control injection comprising Alhydrogel and PBS without antigen. [b] Pneumonic plague is modeled here in mice by infection with virulent wild-type (CO92) and non-encapsulated (C12) *Y. pestis*, as previously established (*16*, *17*). The aerosol LD_{50} values are 6×10^4 CFU for CO92 and 6.8×10^4 CFU for C12. [c] Survival is shown as (number surviving)/(total number exposed). P-values for comparisons of percentage survival are as follows: $p < 0.05$ for groups 1 vs 5, 4 vs 6, 2 vs 5, and 3 vs 6. [d] TTD, time-to-death in days.

Study Objectives. The primary objectives of this investigation were to improve the original design of the fusion protein, engineer a robust purification process, and collect biophysical measurements across production lots pursuant to evaluating the structure of the fusion protein. The secondary objectives of this investigation were to evaluate the protective efficacy of the fusion protein as vaccine antigen against bubonic and pneumonic plague and then compare its protective efficacies to the original F1-V fusion protein and other formulations containing the subcomponent proteins F1 and V. Central to the creation of a robust biological product is the demonstration of a consistent biophysical form among different production lots of pure product. This is particularly true for recombinant proteins manufactured in high yield since such molecules often misfold and coalesce into insoluble derivatives, particularly if hydrophobic or strongly charged (*48*). Both the expression and the purification of F1-V protein were engineered with current FDA guidelines in mind so as to better position the fusion protein antigen for development as a biologic substance and eventual use in humans. The gene fusion was trimmed to express known antigenic structures while minimizing the presence of extraneous or nonnatural amino acids in the original fusion, including F1 leader sequence, purification tags, and protease recognition sites for in-process cleavage. Although often helpful at the research level for protein purification and even expression, tags and their associated proteases add business risk and cost burden to GMP production in the form of testing and controls for product purity and necessitate additional study to document their impact on safety, as residual contaminants, and on functional efficacy as nonessential components. Indeed, even sophisticated expression and purification designs that leave behind few or no unnatural amino acids, such as protease-cleavable sequences or self-excisable inteins, invoke additional regulatory oversight for the same reasons. Furthermore, tags and their residual elements are known to affect

protein folding. A protein production workshop sponsored by The National Institutes of Health Protein Structure Initiative concluded that the overall success rate for proper folding to obtain atomic structure by X-ray crystallography was almost twice as high with native proteins produced without His tags (41%) than with proteins in which the tags had been removed (25%) (*49*). Such burden and risk could not be justified for the new plague vaccine, and instead we chose to design a clean F1-V protein without the use of tags. Kanamycin was used instead of ampicillin for plasmid selection and maintenance during cell banking and fermentation, per FDA guidelines. Although two other expression systems were tested on the basis of presumed benefits of reduced proteolysis (*E. coli* HMS strain) or convertibility to industrial production (*P. pastoris*), the original *E. coli* strain background produced protein of better quality and yield (Figure 2) and was therefore selected as the expression platform from which to develop of a robust purification process. Ample induction of F1-V protein was obtained by the familiar T7 RNA polymerase and IPTG-inducible *placUV5* control of the pET expression system. Additionally, using these popular vectors further reduces future risk because product manifests are publicly available, and they have been used to manufacture biologic substances for other investigational new drug (IND) products. Source ingredients were also evaluated for more direct transfer to industrial scale and eventual GMP production. Importantly, growth media free of animal products functioned equally well as compared to standard media containing tryptone and were therefore used so as to eliminate inadvertent BSE contamination (*32*).

Protein Antigen Production. F1-V protein was isolated through a four-column process that produced 10 mg at 99% final purity per liter of fermentation culture. To maximize the availability of starting material, the first stages of the optimized process employed mechanical cell disintegration in alkaline buffer and then protein denaturation with on-column refolding, thereby recovering nearly one-fourth of the original F1-V at a 3-fold increase in purity (Table 2). This technique substituted well for an earlier research-scale lysis using commercial detergents to scout F1-V expression strains. Alkaline renaturation and on-column refolding were adapted from published procedures due to their successes for the expression and refolding of other insoluble recombinant proteins (*36*, *38*, *50*, *51*). Nevertheless, apparently much of the uncaptured F1-V was in an aggregated form that did not bind the column, and the first step represented the greatest single loss of F1-V throughout the process (Table 2). We could increase this yield by replacing AEX with HIC as the first chromatographic column, but this simply shifted equivalent losses to subsequent procedures (Powell, B. and Enama, J., unpublished results). Unlike the typical behavior of many proteins, F1-V precipitated and was thereafter unrecoverable after holding on ice, salt fractionation, or membrane ultrafiltration. We experienced inordinate losses by these techniques and soon realized that aggregation was the primary difficulty to overcome. Pilot tests with detergents at low concentration did not increase F1-V solubility or prevent aggregation. Using additional chemicals would have added requirements for their removal, testing, and control as contaminants, the evaluation of which was deferred to product development in an industrial manufacturing environment. Instead, operations in high buffer pH and at room temperature functioned well enough to minimize F1-V aggregation and were applied throughout purification. Although 99% purity was achieved after the second chromatographic step, two additional procedures were required to concentrate and exchange F1-V into the desired holding buffer. The optimized finishing steps, steps 3 and 4, returned a combined 51% recovery, with a final yield of 10% after the entire process. This final yield is comparable to production yields reported for other recombinant proteins. Additional effort to overcome these losses by altering fermentation or by introducing additives such as detergents or chaotropic chemicals that may prevent F1-V self-association were also deferred to process development in a professional manufacturing industry setting. While DPBS is not an optimal buffer for frozen storage because of the differential affect of cold temperature on the lower pK_a's of phosphate ion, it was employed without stabilizer or preservative to store F1-V antigen for direct thaw-and-use in animal studies and for consistency in comparing to historical results (*16*, *17*, *19*). The tendency for aggregation increased with purity, and once thawed from frozen storage, soluble F1-V did not withstand repeated freezing and thawing, extended hold times at cold temperature, rapid changes in pH, or increased salt content. Such properties were first observed for purified recombinant F1 protein (*15*). A commercially prepared lot of F1-V purified by a modified process was donated to USAMRIID for biophysical and biological comparability studies. This material was concentrated to 1 mg/mL and buffer exchanged into DPBS prior to freezing and use. Later bridging studies (Powell, B. and Andrews, G., unpublished data) confirmed equivalency in structure and protective efficacy to the standard F1-V lots produced at USAMRIID and described here. This indicated that the F1-V fusion protein antigen was itself a robust biological substance, since similar final structures and protective efficacies were achieved through three different methods of purification.

Fusion Protein Characterization. Several biochemical and biophysical methods were used to characterize the structure of F1-V and to qualify it for use in animal studies. SDS−PAGE, immunoblots, and CIEF all verified that the purified protein had a relative molecular size and measured pI as would be expected for the putative translation product of the engineered gene fusion (Figures 1−3 and 6). However, while confirming protein identity, Edman sequencing and then time-of-flight and electrospray mass spectrometry revealed that its N-terminal translation initiator Met was absent, leaving the penultimate amino acid Ala at the terminus (Figures 1, 4, and 5). Methionine aminopeptidase cleaves the N-terminal Met for most of the nascent translation products in *E. coli*, and enzymatic activity is affected by residues neighboring the initiator methionine. It is important to define the amino terminus of a purified recombinant protein since the des-Met form is often crucial for protein function and stability (*52*). In this regard, similar confirmation for a cocktail vaccine would be required to define the primary structures of F1 protein, expressed in *E. coli* from a subcloned *Y. pestis caf* operon with assumed processing of its natural leader peptide sequence (*15*), and for recombinant V, whose tagged gene fusion was cleaved in vitro but retains unnatural N-terminal amino acids. Because no other post-translational modifications were detected in this study, these results established that the purified F1-V fusion protein was a des-Met product of 477 amino acids and 53,061 Da. Gel densitometry was the most reliable method we found for measuring F1-V purity because the protein fractionated into a wide range of higher-order forms by SEC-HPLC in DPBS buffer (Figure 11), it had an A_{280} that was too low to be useful for direct measure-

ment or for comparison to protein contaminants, and it was largely refractory to standard conditions for RP-HPLC. Nevertheless, different lots of F1-V produced similar chromatograms by the RP-HPLC method developed here for F1-V, further indicating that the purification and folding process is consistent (Figure 7). Similarity in tryptophan fluorescence and CD spectroscopic spectra among lots provided supporting evidence of proper protein folding (Figures 8 and 9). Because predicted and observed secondary structures are concordant and because spectra are consistent among several lots and between two production methods, it appears that F1-V fusion protein assumes its lowest-energy conformation and folds properly through this procedure. Reproducible spectra were also observed for intrinsic fluorescence measurements of tertiary structure. Again, it is unlikely that the fusion protein had consistently misfolded among different purification methods and lots. Hence, we conclude that F1-V protein folds properly and reproducibly as measured by first principles, supported by theoretical calculations, and verified by surveying protein isolated by two nonidentical methods and across several production lots. We observed variations in higher-order structure between lots of F1-V while developing an SEC-MALS assay (Figure 11) for use as a measure of protein quaternary structure and indicator of product quality. Measurements in DPBS at 37 °C showed that purified F1-V comprises a polydisperse population of soluble forms ranging in size from the monomeric molecule to soluble aggregates over 1.5×10^7 Da. Every lot tested under these conditions contained a predominant peak of averaged mass near 2.12×10^5 Da, corresponding to a tetramer of F1-V molecules (Figure 11). Interestingly, under these same conditions the smaller F1 protein forms an aggregate of maximum size 10 times greater than that of F1-V (Figure 11). The predominant bulk form of F1 has an averaged mass near 3×10^6 Da, equivalent to approximately 200 molecules in comparison to the tetramer formed by F1-V under these conditions. In contrast, purified rV protein contains very little aggregation but varies in the relative distribution of monomeric and dimeric forms depending on the expression clone and production method (data not shown). The SEC-MALS assay conditions of 37 °C in buffer of physiological pH and salinity were chosen so as to observe protein structure under conditions that mimic the body after administration. Colder temperatures resembling a theoretical bed-side hold on ice could not be tested; however, measurements at 25 °C revealed a disproportionate shift in all structures to higher maximum and bulk masses for both F1-V and F1. Notably, the fusion protein was less affected by cold temperature than was the F1 protein. Since F1 was the primary component of the Plague Vaccine USP, our data here suggests that the variable insolubility of F1 protein may have contributed to known difficulties in manufacture of the vaccine as well as to difficulties in achieving consistent immunization results for which a dependable universal dosing regimen was never established. Therefore, F1-V is a more robust vaccine antigen than is a saline suspension of F1 as contained in the Plague Vaccine USP. Thus, the F1-V fusion protein containing two whole antigens in a single substance has a better defined primary composition, more consistent higher-order structure, and increased stability and is at least equivalent in protective efficacy as compared to the former licensed vaccine or a proposed cocktail vaccine of individual recombinant F1 and V protein antigens.

Vaccine Efficacy. The data reported herein verify that the redesigned F1-V antigen confers high protection against bubonic and pneumonic plague in mice and causes high circulating antibody titers to both F1 and V proteins (Tables 5 and 6). Importantly, the improved vaccine antigen provides very good protection against extremely high-level aerosol challenges by both normal and non-encapsulated virulent *Y. pestis* strains (Table 6), as was shown previously for the original fusion (*16*, *17*). Therefore, the present results and historical findings establish statistical equivalency between the improved fusion protein and the original His-tagged fusion for protective efficacy in the bubonic and pneumonic plague models. This work also reconfirms the previously reported relationship (*16*, *17*) that the original fusion protein architecture provides higher protective efficacy than the Plague Vaccine USP (Table 4) and establishes with statistical significance the observed difference between the two vaccines. Thus, the basic fusion protein design provides several thousand-fold better protective efficacy (5,750×) against bubonic plague than does the Plague Vaccine USP. By the same analysis, this work also provides new statistical significance to another relationship described previously (*16*, *17*): that related nonfusion formulations confer much higher protective efficacy against plague than USP, including the individual V protein (500×) and a cocktail of F1 and V antigens (1150×) (Table 3). This concurs with an independent study that tested a cocktail vaccine comprising a 2:1 protein molar ratio of F1 and V (*42, 44*, *53*). However, at this vaccine dose and in this mouse model with these challenge levels, the current data further demonstrate that the fusion protein architecture provides statistically better protection against lethal challenge from wild-type *Y. pestis* than does the F1 + V cocktail design (Table 3). Finally, these findings quantify a previously reported (*53*, *60*) synergistic effect of simultaneous immunization with both F1 and V antigens, since both the fusion and cocktail vaccines are statistically more potent than vaccination with either individual subcomponent protein (Table 3).

With regard to induction of specific immunity, these data show that the USP vaccine elicits relatively little anti-F1 activity and no anti-V activity, whereas the F1 and V formulations, including both fusion protein constructs, all provide very high circulating titers to the respective protective antigens delivered, as reported previously (*16*, *17*, *53*). That the Plague Vaccine USP induces relatively little pre-challenge anti-F1 immunity as compared to immunization with purified recombinant F1 (Table 4) has been observed previously (*17*). Although a cause for this difference in immunogenicity was not directly tested, we suggest the variable quantity and quality of F1 in the former USP vaccine may account for part of the discrepancy, noting that the amount of F1 protein in the former vaccine was observed to vary 10-fold among tested lots and the apparent mass of its F1 protein component appeared larger than that of recombinant F1 protein (*17*, Andrews, G., unpublished data). The formaldehyde-fixed and killed whole cells are known to contain immunomodulators, such as lipopolysaccharide, and may also have other undefined effectors of immunity. Moreover, the cell suspension settles from solution and may vary in total content among lots and between uses. These explanations are concordant with its known variability in quality, time to immunity, and protective efficacy as documented epidemiologically in humans (40, 41) and experimentally in animal studies (*15*−*17*, *41*, *42*, *53*). By the current analysis, however,

the apparent differences in anti-F1 immune titers are not statistically significant (Table 4, footnote b) and therefore do not directly answer a separate interest to define a measurable correlate of protective immunity. Nevertheless, such assays have been defined (*53*), and humoral immunity conferred by these antigens has previously been established by passive protection against plague after transfer of immune sera or IgG (*53*−*57*). Thus, these findings establish equivalency in protective efficacy between prior and new F1-V fusion proteins and thereby demonstrate the intended improvement in biological activity over the former licensed USP vaccine, while also showing higher efficacy by either fusion protein in direct comparisons to related formulations containing these protective antigens, including an F1 + V cocktail vaccine.

Conclusions

We have re-engineered, expressed, purified, tested, and compared an improved, non-tagged form of the F1-V fusion protein antigen to better position it as a robust biological substance for development of the new plague vaccine. Our structural characterizations demonstrate that the recommended research-level purification process is reproducible and yields F1-V protein of consistent secondary and tertiary structure, concordant with proper protein folding and supporting the notion that the subcomponent proteins retain much of their natural secondary and tertiary structures as folded within the protein fusion. This work establishes that the observed tendency for the fusion protein to aggregate is caused by a natural property of the F1 subcomponent protein. Importantly, the fusion protein architecture reduces aggregation at least 10-fold compared to isolated F1 protein and thereby decreases product heterogeneity relative to alternative vaccine formulations containing separate antigens. Finally, we have demonstrated that F1-V functions very well as a protective antigen against both bubonic and pneumonic plague, having efficacy that is equivalent to that of the prior fusion antigen and far better than that provided by the former licensed Plague Vaccine USP. In simultaneous comparisons of related antigen vaccine formulations, the fused F1-V protein architecture provided statistically better protection in this bubonic plague model than did a cocktail of separate F1 and V proteins. In summary, these findings verify that the recombinant F1-V fusion protein design and research level purification process described herein provide a robust and effective platform for the creation of a multicomponent protective antigen and establish that this improved F1-V substance is well suited for development as the active ingredient of the next plague vaccine.

Acknowledgment

We thank J. Farchaus, S. Strachan, and G. Anderson for help during early design and testing; S. Cox, R. Cushman, M. McClain, S. Hebert, N. Parthasarathy, J. Jackman, and J. Schmidt for laboratory assistance and services; and S. Norris and P. Gibbs for statistical calculations. We also thank J. Pace-Templeton, L. Taylor, and C. Nielsen (OPDRA, USAMRIID), V. Pierson (JVAP), and D. Snow, B. Solo, and S. Morris (DVC) for helpful guidance during the development and transfer of product materials and technology from USAMRIID to JVAP, DVC, and subcontractors. Disclaimer in accordance with AR 70-31: opinions, interpretations, conclusions, and recommendations are those of the authors and are not necessarily endorsed by the U.S. Army. This work was supported in part by USAMRIID research projects 02-4-AA-001 and 02-4-AA-004 to B. Powell.

References and Notes

(1) Abbreviations used: Ab, antibody; AEX, anion exchange chromatography; CEX, cation exchange chromatography; CIEF, capillary isoelectric focusing; des-Met, without the N-terminal translation initiator methionine; DO_2, dissolved oxygen; DPBS, Dulbecco's phosphate-buffered saline without Ca^{2+} or Mg^{2+}; F1-V, fusion protein comprising *Y. pestis* fraction 1 capsule joined to V antigen; FDA, Food and Drug Administration; GMP, good manufacturing practices; GMT, geometric mean titer; GSD, geometric standard deviation; HPLC, high-pressure liquid chromatography; IEP, isoelectric point; IPTG, isopropyl-β-D-thiogalactoside; KWC, killed whole cell; LD_{50}, 50% lethal dose; MALDI-TOF-MS, matrix-assisted laser desorption ionization time-of-flight mass spectrometry; Met, methionine; M_r, relative molecular weight; MST, mean survival time as measured in days; *m/z*, mass-to-charge; OD_{405}, optical density at 405 nm wavelength; PCR, polymerase chain reaction; RFLP, restriction fragment length polymorphism; RP-HPLC, reversed-phase high-pressure liquid chromatography; SC, subcutaneous; SE, standard error; SEC, size exclusion chromatography; SEC-MALS, size exclusion chromatography coupled to multi-angle light scattering spectroscopy; Tet^R, tetracycline resistance; USAMRIID, United States Army Medical Research Institute of Infectious Diseases; YOP, *Yersinia* outer protein.

(2) Achtman, M.; Morelli, G.; Zhu, P.; Wirth, T.; Diehl, I.; Kusecek, B.; Vogler, A. J.; Wagner, D. M.; Allender, C. J.; Easterday, W. R.; Chenal-Francisque, V.; Worsham, P.; Thomson, N. R.; Parkhill, J.; Lindler, L. E.; Carniel, E.; Keim, P. Microevolution and history of the plague bacillus, *Yersinia pestis*. *Proc. Natl. Acad. Sci. U.S.A.* **2004**, *101*, 17837−17842.

(3) Adair, D. M.; Worsham, P. L.; Hill, K. K.; Klevytska, A. M.; Jackson, P. J.; Friedlander, A. M.; Keim, P. Diversity in a variable-number tandem repeat from *Yersinia pestis*. *J. Clin. Microbiol.* **2000**, *38*, 1516−9.

(4) Hinnebusch, B. J. Transmission factors: *Yersinia pestis* genes required to infect the flea vector of plague. *Adv. Exp. Med. Biol.* **2003**, *529*, 55−62.

(5) Hinnebusch, B. J. Bubonic plague: a molecular genetic case history of the emergence of an infectious disease. *J. Mol. Med.* **1997**, *75*, 645−652.

(6) Perry, R. D.; Fetherston, J. D. *Yersinia pestis*—etiologic agent of plague. *Clin. Microbiol. Rev.* **1997**, *10*, 35−66.

(7) Plague, WHO Fact Sheet No. 267, Revised February 2005; http://www.who.int/mediacentre/factsheets/fs267/en/.

(8) Galimand, M.; Guiyoule, A.; Gerbaud, G.; Rasoamanana, B.; Chanteau, S.; Carniel, E.; Courvalin, P. Multidrug resistance in *Yersinia pestis* mediated by a transferable plasmid. *New Engl. J. Med.* **1997**, *337*, 677−680.

(9) Guiyoule, A.; Gerbaud, G.; Buchrieser, C.; Galimand, M.; Rahalison, L.; Chanteau, S.; Courvalin, P.; Carniel, E. Transferable plasmid-mediated resistance to streptomycin in a clinical isolate of *Yersinia pestis*. *Emerging Infect. Dis.* **2001**, *7*, 43−48.

(10) Inglesby, T. V.; Dennis, D. T.; Henderson, D. A.; Bartlett, J. G.; Ascher, M. S.; Eitzen, E.; Fine, A. D.; Friedlander, A. M.; Hauer, J.; Koerner, J. F.; Layton, M.; McDade, J.; Osterholm, M. T.; O'Toole, T.; Parker, G.; Perl, T. M.; Russell, P. K.; Schoch-Spana, M.; Tonat, K. Plague as a biological weapon: medical and public health management. Working Group on Civilian Biodefense. *JAMA*, *J. Am. Med. Assoc.* **2000**, *283*, 2281−2290.

(11) McGovern, T.; Faad, M.; Friedlander, A. Plague. In *Medical Aspects of Chemical & Biological Warfare, Part I*; Sidell, F., Takafuji, E., Franz, D., Eds.; Office of the Surgeon General: Washington, DC, 1997; Vol. 23, pp 479−502.

(12) McGovern, T. W.; Christopher, G. W.; Eitzen, E. M. Cutaneous manifestations of biological warfare and related threat agents. *Arch. Dermatol.* **1999**, *135*, 311−322.

(13) Davis, J.; Johnson-Winegar, A. The anthrax terror: DOD's number-one biological threat. *Aerospace Power J.* **2000**, *xiv*, 15−29.

(14) Alibek, K.; Handelman, S. *Biohazard: The Chilling True Story of the Largest Covert Biological Weapons Program in the World*; Random House: New York, 1999.
(15) Andrews, G. P.; Heath, D. G.; Anderson, G. W., Jr.; Welkos, S. L.; Friedlander, A. M. Fraction 1 capsular antigen (F1) purification from *Yersinia pestis* CO92 and from an *Escherichia coli* recombinant strain and efficacy against lethal plague challenge. *Infect. Immun.* **1996**, *64*, 2180−2187.
(16) Anderson, G. W., Jr.; Heath, D. G.; Bolt, C. R.; Welkos, S. L.; Friedlander, A. M. Short- and long-term efficacy of single-dose subunit vaccines against *Yersinia pestis* in mice. *Am. J. Trop. Med. Hyg.* **1998**, *58*, 793−799.
(17) Heath, D. G.; Anderson, G. W., Jr.; Mauro, J. M.; Welkos, S. L.; Andrews, G. P.; Adamovicz, J.; Friedlander, A. M. Protection against experimental bubonic and pneumonic plague by a recombinant capsular F1-V antigen fusion protein vaccine. *Vaccine* **1998**, *16*, 1131−1137.
(18) Anderson, G. W., Jr.; Leary, S. E.; Williamson, E. D.; Titball, R. W.; Welkos, S. L.; Worsham, P. L.; Friedlander, A. M. Recombinant V antigen protects mice against pneumonic and bubonic plague caused by F1-capsule-positive and -negative strains of *Yersinia pestis*. *Infect. Immun.* **1996**, *64*, 4580−4585.
(19) Benner, G. E.; Andrews, G. P.; Byrne, W. R.; Strachan, S. D.; Sample, A. K.; Heath, D. G.; Friedlander, A. M. Immune response to *Yersinia* outer proteins and other *Yersinia pestis* antigens after experimental plague infection in mice. *Infect. Immun.* **1999**, *67*, 1922−1928.
(20) Jackson, M. W.; Plano, G. V. Interactions between type III secretion apparatus components from *Yersinia pestis* detected using the yeast two-hybrid system. *FEMS Microbiol. Lett.* **2000**, *186*, 85−90.
(21) Brubaker, R. R. The V antigen of yersiniae: an overview. *Contrib. Microbiol. Immunol.* **1991**, *12*, 127−133.
(22) Sing, A.; Rost, D.; Tvardovskaia, N.; Roggenkamp, A.; Wiedemann, A.; Kirschning, C. J.; Aepfelbacher, M.; Heesemann, J. Yersinia V-antigen exploits toll-like receptor 2 and CD14 for interleukin 10-mediated immunosuppression. *J. Exp. Med.* **2002**, *196*, 1017−1024.
(23) Williamson, E. D.; Eley, S. M.; Stagg, A. J.; Green, M.; Russell, P.; Titball, R. W. A subunit vaccine elicits IgG in serum, spleen cell cultures and bronchial washings and protects immunized animals against pneumonic plague. *Vaccine* **1997**, *15*, 1079−1084.
(24) Tartof, K. D.; Hobbs, C. A. New cloning vectors and techniques for easy and rapid restriction mapping. *Gene* **1988**, *67*, 169−82.
(25) Price, S. B.; Leung, K. Y.; Barve, S. S.; Straley, S. C. Molecular analysis of lcrGVH, the V antigen operon of *Yersinia pestis*. *J. Bacteriol.* **1989**, *171*, 5646−5653.
(26) Potter, K. J.; Bevins, M. A.; Vassilieva, E. V.; Chiruvolu, V. R.; Smith, T.; Smith, L. A.; Meagher, M. M. Production and purification of the heavy-chain fragment C of botulinum neurotoxin, serotype B, expressed in the methylotrophic yeast *Pichia pastoris*. *Protein Expression Purif.* **1998**, *13*, 357−365.
(27) Labarca, C.; Paigen, K. A simple, rapid, and sensitive DNA assay procedure. *Anal. Biochem.* **1980**, *102*, 344−352.
(28) Combet, C.; Blanchet, C.; Geourjon, C.; Deleage, G. NPS@: network protein sequence analysis. *Trends Biochem. Sci.* **2000**, *25*, 147−150; application available at http://npsa-pbil.ibcp.fr.
(29) Takach, E. J.; Hines, W. M.; Patterson, D. H.; Juhasz, P.; Falick, A. M.; Vestal, M. L.; Martin, S. A. Accurate mass measurements using MALDI-TOF with delayed extraction. *J. Protein Chem.* **1997**, *16*, 363−369.
(30) Goodin, J. L.; Raab, R. W.; McKown, R. L.; Coffman, G. L.; Powell, B. S.; Enama, J. T.; Ligon, J. A.; Andrews, G. P. *Yersinia pestis* outer membrane type III secretion protein YscC: expression, purification, characterization, and induction of specific antiserum. *Protein Expression Purif.* **2005**, *40* (1), 152−163.
(31) *Guide for the Care and Use of Laboratory Animals*; National Academy Press: Washington, DC, 1996; p 116. Accessible from http://www.nap.edu/readingroom/books/labrats/.
(32) Bovine Spongiform Encephalopathy (BSE), U.S. Food and Drug Administration Center for Biologics Evaluation and Research, and references therein, http://www.fda.gov/cber/bse/bse.htm, accessed 31 March 2005.
(33) Fischer, B. E. Renaturation of recombinant proteins produced as inclusion bodies. *Biotechnol. Adv.* **1994**, *12*, 89−101.
(34) Margalit, H.; Fischer, N.; Ben-Sasson, S. A. Comparative analysis of structurally defined heparin binding sequences reveals a distinct spatial distribution of basic residues. *J. Biol. Chem.* **1993**, *268*, 19228−19231.
(35) Farchaus, J. W.; Ribot, W. J.; Jendrek, S.; Little, S. F. Fermentation, purification, and characterization of protective antigen from a recombinant, avirulent strain of *Bacillus anthracis*. *Appl. Environ. Microbiol.* **1998**, *64*, 982−991.
(36) Suttnar, J.; Dyr, J. E.; Hamsikova, E.; Novak, J.; Vonka, V. Procedure for refolding and purification of recombinant proteins from *Escherichia coli* inclusion bodies using a strong anion exchanger. *J. Chromatogr., B: Biomed. Sci. Appl.* **1994**, *656*, 123−6.
(37) Cowley, D. J.; Mackin, R. B. Expression, purification and characterization of recombinant human proinsulin. *FEBS Lett*. **1997**, *402*, 124−130.
(38) Jungbauer, A.; Kaar, W.; Schlegl, R. Folding and refolding of proteins in chromatographic beds. *Curr. Opin. Biotechnol.* **2004**, *15*, 487−494.
(39) Li, M.; Su, Z. G.; Janson, J. C., In vitro protein refolding by chromatographic procedures. *Protein Expression Purif.* **2004**, *33*, 1−10.
(40) Marshall, J. D., Jr.; Bartelloni, P. J.; Cavanaugh, D. C.; Kadull, P. J.; Meyer, K. F. Plague immunization. II. Relation of adverse clinical reactions to multiple immunizations with killed vaccine. *J. Infect. Dis.* **1974**, *129*, (Suppl) S19−S25.
(41) Meyer, K. Effectiveness of live or killed plague vaccines in man. *Bull. WHO* **1970**, *42*, 653−666.
(42) Williamson, E. D.; Eley, S. M.; Griffin, K. F.; Green, M.; Russell, P.; Leary, S. E.; Oyston, P. C.; Easterbrook, T.; Reddin, K. M.; Robinson, A. et al. A new improved subunit vaccine for plague: the basis of protection. *FEMS Immunol. Med. Microbiol.* **1995**, *12*, 223−230.
(43) Biological products; bacterial vaccines and toxoids, implementation of efficacy review. *Fed. Regist.* **2004**, *29* (249), 78281−78293; available at http://www.fda.gov/OHRMS/DOCKETS/98fr/04-28322.htm.
(44) Williamson, E. D.; Eley, S. M.; Stagg, A. J.; Green, M.; Russell, P.; Titball, R. W. A single dose subunit vaccine protects against pneumonic plague. *Vaccine* **2000**, *19* (4−5), 566−71.
(45) Shapiro, S. Z. The HIV/AIDS vaccine researchers' orientation to the process of preparing a U.S. FDA application for an investigational new drug (IND): what it is all about and how you start by preparing for your pre-IND meeting. *Vaccine* **2002**, *20* (9−10), 1261−1280.
(46) New drug and biological drug products; evidence needed to demonstrate effectiveness of new drugs when human efficacy studies are not ethical or feasible. *Fed. Regist.* **2002**, *29* (105), 37988−37998; available at http://www.fda.gov/OHRMS/DOCKETS/98fr/053102a.htm.
(47) Andrews, G. P.; Strachan, S. T.; Benner, G. E.; Sample, A. K.; Anderson, G. W., Jr.; Adamovicz, J. J.; Welkos, S. L.; Pullen, J. K.; Friedlander, A. M. Protective efficacy of recombinant *Yersinia* outer proteins against bubonic plague caused by encapsulated and non-encapsulated *Yersinia pestis*. *Infect. Immun.* **1999**, *67*, 1533−1537.
(48) Cutler, P. In *Protein Purification Protocols*, 2nd ed.; Walker, J. M., Ed.; Humana Press: Totowa, NJ, 2004; pp 29−35.
(49) Protein structure initiative, protein production workshop. National Institute of General Medical Sciences, Mar 7−8, 2002; available at http://www.nigms.nih.gov/news/reports/protein_production.html#session1.
(50) Fischer, B.; Perry, B.; Sumner, I.; Goodenough, P. A novel sequential procedure to enhance the renaturation of recombinant protein from *Escherichia coli* inclusion bodies. *Protein Eng.* **1992**, *5*, 593−596.
(51) Sijwali, P. S.; Brinen, L. S.; Rosenthal, P. J. Systematic optimization of expression and refolding of the *Plasmodium*

falciparum cysteine protease falcipain-2. *Protein Expression Purif.* **2001**, *22*, 128−134.
(52) Ben-Bassat, A.; Bauer, K.; Chang, S. Y.; Myambo, K.; Boosman, A.; Chang, S. Processing of the initiation methionine from proteins: properties of the *Escherichia coli* methionine aminopeptidase and its gene structure. *J. Bacteriol.* **1987**, *169*, 751−757.
(53) Williamson, E. D.; Vesey, P. M.; Gillhespy, K. J.; Eley, S. M.; Green, M.; Titball, R. W. An IgG1 titre to the F1 and V antigens correlates with protection against plague in the mouse model. *Clin. Exp. Immunol.* **1999**, *116*, 107−114.
(54) Casadevall, A. Passive antibody administration (immediate immunity) as a specific defense against biological weapons. *Emerging Infect. Dis.* **2002**, *8*, 833−841.
(55) Anderson, G. W.; Worsham, P. L.; Andrews, G. P.; Bolt, C. R.; Welkos, S. L.; Friedlander, A. M.; Burans, J. P. Passive immunization with monoclonal antibodies against the F1 antigen of *Yersinia pestis* protects mice from fatal bubonic and pneumonic plague. Conference poster at the American Society of Tropical Medicine & Hygiene, San Antonio, TX, 20 November 1995.
(56) Andrews, G. P.; Bolt, C. R.; Pitt, L. M.; Adamovicz, J. J. Passive protection in mice from fatal pneumonic plague by antibody raised against a recombinant *Yersinia pestis* F1-V fusion protein vaccine candidate. Poster at American Society for Microbiology 104th General Meeting, 2004.
(57) Une, T.; Brubaker, R. R. Roles of V antigen in promoting virulence and immunity in yersiniae. *J. Immunol.* **1984**, *133*, 2226−30.
(58) Welkos, S. L.; Davis, K. M.; Pitt, L. M.; Worsham, P. L.; Freidlander, A. M. Studies on the contribution of the F1 capsule-associated plasmid pFra to the virulence of *Yersinia pestis*. *Contrib. Microbiol. Immunol.* **1995**, *13*, 299−305.
(59) Worsham, P. L.; Stein, M. P.; Welkos, S. L. Construction of defined F1 negative mutants of virulent *Yersinia pestis*. *Contrib. Microbiol. Immunol.* **1995**, *13*, 325−328.
(60) Hill, J.; Copse, C.; Leary, S.; Stagg, A. J.; Williamson, E. D.; Titball, R. W. Synergistic protection of mice against plague with monoclonal antibodies specific for the F1 and V antigens of *Yersinia pestis*. *Infect. Immun.* **2003**, *71*, 2234−2238.

Accepted for publication June 27, 2005.

BP050098R